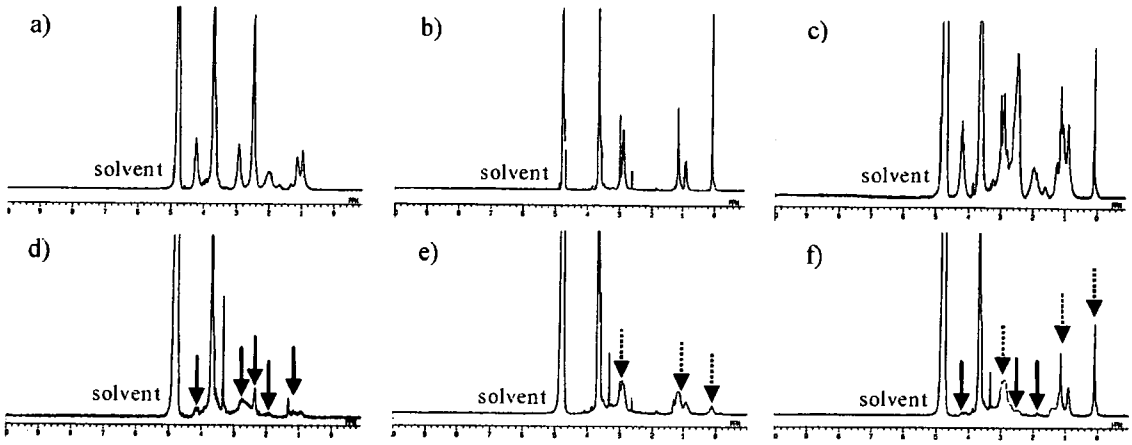

Figure 7. ^{1}H NMR spectra of (a) the Lac-PEG-PAMA block copolymer at pD = 7.4, (b) the Lac-PEG-PSAO block copolymer at pD = 7.4, (c) Lac-PEG-PSAO-PAMA triblock copolymer at pD = 7.4, (d) the Lac-PEG-PAMA/pDNA polyplex micelle at pD = 7.4, (e) the Lac-PEG-PSAO/pDNA polyplex micelle at pD = 7.4, and (f) the Lac-PEG-PSAO-PAMA/pDNA polyplex micelle at pD = 7.4 in D_2O containing 0.15 M NaCl at 37 °C. The solid and dotted arrows indicate the peaks corresponding to the PAMA segment and PSAO segment, respectively.

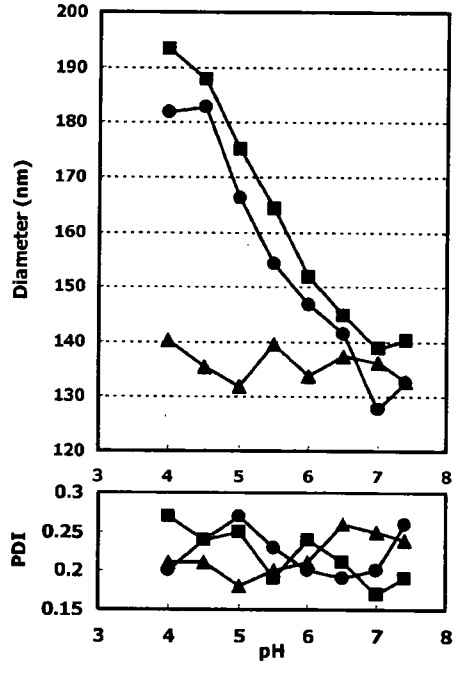

Figure 8. pH vs diameter (d) and PDI (μ_2/Γ^2) of the Lac-PEG-PSAO-PAMA/pDNA (circle), Lac-PEG-PAMA/pDNA (triangle), and Lac-PEG-PSAO/pDNA (square) polyplex micelles at N/P = 3 (angle, 90°; solvent, distilled water including 0.15 M NaCl; temperature, 37 °C).

micelle may induce the selective expansion of the PSAO inner shell while retaining the condensed pDNA in the PAMA/pDNA PIC core, leading to the remarkable pH-induced size variation. However, the observed size variation is clearly too large compared with the calculated PSAO length as the fully stretched chains for coil-state (pH 7.4) and rod-state (pH 4.0), indicating that the expansion of the PSAO inner shell is not sufficient to account for the size variation of the micelles. Although other possible factors probably exist, we believe that the expansion of the PSAO inner shell is one of the factor for the size variation of the micelles. On the other hand, the peaks from the PSAO segment clearly appeared in the ^{1}H NMR spectrum of the Lac-PEG-PSAO/pDNA polyplex micelle at pD = 4.0, suggesting that the conformational changes (globule-rod transition) of the complexed PSAO segment in the Lac-PEG-PSAO/pDNA polyplex micelle presumably leads to the formation of a loose PIC core (see Supporting Information). Apparently, the high rigidity of the protonated PSAO chain in the lower pH region should be unfavorable for triggering the DNA condensation upon complexation. As a consequence, a loose complex may form between pDNA and the PSAO segment without condensation in the lower pH region, showing an appreciable size increase.

Evaluation of the Biological Efficacy of the Polyplex Micelles. The cytotoxicity of the Lac-PEG-PSAO-PAMA, Lac-PEG-PAMA, and Lac-PEG-PSAO block copolymers against HuH-7 cells (hepatocytes) was studied using an MTT assay (see: Supporting Information). The viability of cells treated with the Lac-PEG-PSAO block copolymer was less than 20% at a polymer concentration of 100 μg/mL (IC_{50} < 30 μg/mL). In contrast, cells incubated with Lac-PEG-PSAO-PAMA or Lac-PEG-PAMA retained 65~70% viability relative to controls even at concentrations up to 100 μg/mL. This result indicates that the inclusion of PSAO segment into the Lac-PEG-PSAO-PAMA triblock copolymer seems to substantially reduce its inherent cytotoxicity.

To examine whether the lactose moiety (galactose terminal) on the surface of Lac-PEG-PSAO-PAMA/pDNA polyplex micelle is recognized by the asialoglycoprotein (ASGP) receptors existing on the HuH-7 cells (*34*, *35*), the cellular association and internalization of the polyplex micelle (N/P = 3) with fluorescein isothiocyanate (FITC)-labeled pDNA were visualized under a fluorescence microscope at 60 min of incubation in the presence and absence of asialofetuine (ASF). Note that the ASF is known to function as a competitive inhibitor for the ASGP receptor-mediated endocytosis (*36*). The cellular association and internalization of the Lac-PEG-PSAO-PAMA/pDNA polyplex micelle to HuH-7 cells in the absence of ASF were clearly observed as shown in Figure 9b,d. On the contrary, substantially reduced cellular association and internalization of the micelles were observed in the presence of ASF as shown in Figure 9a,c. This result indicates that the cellular association and internalization of the Lac-PEG-PSAO-PAMA/pDNA polyplex micelle occur mainly through the ASGP receptor-mediated process, which is inhibited in the presence of ASF (*37*).

To estimate the transfection ability of the Lac-PEG-PSAO-PAMA/pDNA, Lac-PEG-PAMA/pDNA, and Lac-PEG-PSAO/pDNA polyplex micelles with various N/P ratios, a transfection study using HuH-7 cells was carried out in the presence of 10% FBS. A pGL-3 control plasmid DNA encoding firefly luciferase was used as a reporter gene. In addition, the B-PEI/pDNA polyplex was used as a control vector at the optimal N/P ratio of 10 to show the highest transfection efficacy. As shown in Figure 10, the transfection efficiency of the Lac-PEG-PSAO-

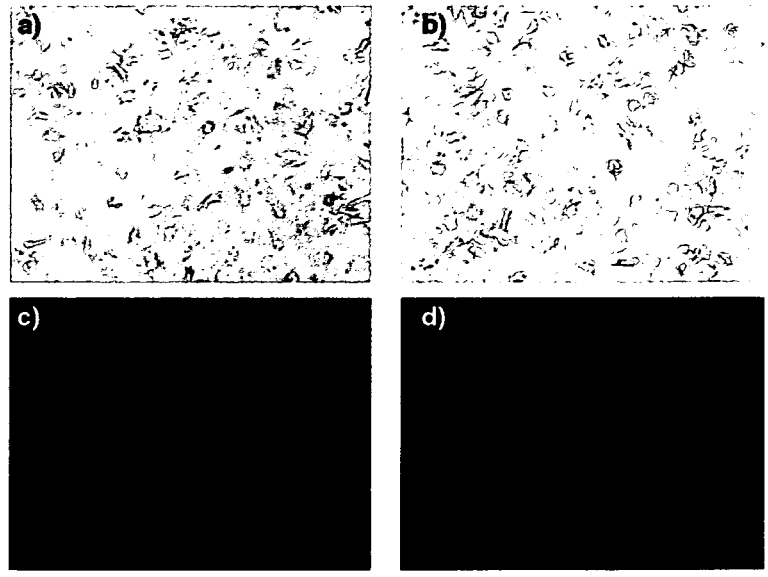

Figure 9. Association and internalization to HuH-7 cells of the Lac-PEG-PSAO-PAMA/pDNA polyplex micelles prepared at N/P = 3 after 60 min incubation. (a) ASF (+) (phase-contrast image), (b) ASF (−) (phase-contrast image), (c) ASF (+) (fluorescent image), and (d) ASF (−) (fluorescent image).

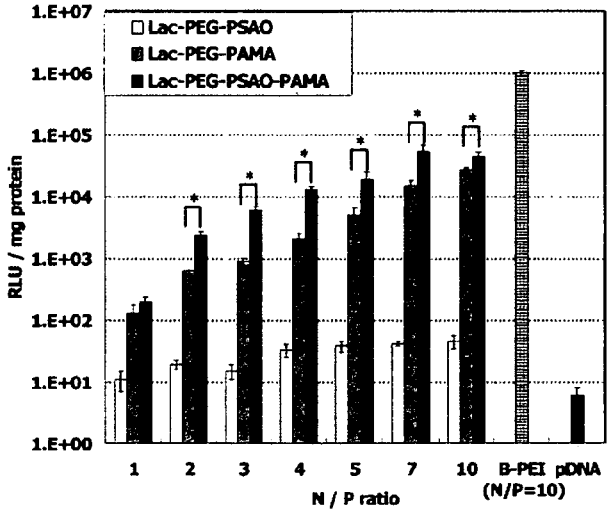

Figure 10. Transfection efficiency to HuH-7 cells of the Lac-PEG-PSAO-PAMA/pDNA, Lac-PEG-PAMA/pDNA, and Lac-PEG-PSAO/pDNA polyplex micelles prepared at various N/P ratios with a fixed pDNA amount. The plotted data are the average of triplicate experiments ± SD ($P^* < 0.05$).

PAMA/pDNA and Lac-PEG-PAMA/pDNA polyplex micelles was substantially improved with an increasing N/P ratio. In particular, 1 order of magnitude increase in transfection efficiency was achieved by increasing the N/P ratio from 1 to 2 ($P < 0.05$), corresponding to the formation of a stable polyplex structure judging from the agarose gel retardation assay, seen in Figure 6. Alternatively, the Lac-PEG-PSAO/pDNA polyplex micelles exhibited only limited transfection efficiency, presumably due to the low DNA condensing capacity of the PSAO chain as indicated from the results of the EtBr exclusion assay shown in Figure 5. Thus, polyplex micelles formed from Lac-PEG-PSAO may not be stable enough to be tolerated in the culture medium containing a substantial amount of serum proteins. Of interest, the transfection efficiency of the Lac-PEG-PSAO-PAMA/pDNA polyplex micelles always revealed a higher transfection efficiency than the Lac-PEG-PAMA/pDNA polyplex micelles in the range of N/P ratios between 2 and 10 ($P < 0.05$).

To determine whether the difference in the transfection efficiency between the Lac-PEG-PSAO-PAMA/pDNA and Lac-PEG-PAMA/pDNA polyplex micelles is related to the endosomal escape function, confocal microscope experiments were performed on the HuH-7 cells treated with the polyplex micelles containing FITC-labeled pDNA. Cells were co-incubated with LysoTracker Red DND-99 probe, which specifically stains acidic organelles such as endosomes and lysosomes. Thus, the colocalization of the polyplex micelles and the LysoTracker Red probe in an acidic compartment (endosome and lysosome) should be detected as yellow (or orange) fluorescence due to the merging of green and red colors. In the case of the Lac-PEG-PAMA/pDNA polyplex micelles (Figure 11a,b), the yellow and red fluorescences were observed without isolated green fluorescence even after a 120-min incubation, indicating that the polyplex micelles localized in the endosomes and/or lysosomes with the LysoTracker Red probe. The Lac-PEG-PSAO-PAMA/pDNA polyplex micelles localized in the endosomes and/or the lysosomes with the LysoTracker Red probe after a 30 min incubation (Figure 11c), as suggested by the partially yellow fluorescence. At 120 min of incubation, diffused green fluorescence was observed in the cytoplasm (Figure 11d), indicating that the Lac-PEG-PSAO-PAMA/pDNA polyplex micelles gradually escaped from the endosomes and/or lysomes into the cytoplasm in a time-dependent manner. These results suggest that both the PAMA segment as a DNA-condensing polycation and the PSAO segment as the buffering moiety may synergistically contribute to enhance the transfection efficiency of the Lac-PEG-PSAO-PAMA/pDNA polyplex micelles. Although the Lac-PEG-PSAO-PAMA/pDNA polyplex micelles showed 1 order of magnitude lower transfection efficiency than the B-PEI/pDNA polyplex at N/P = 10 ($P < 0.05$), this value may still be appreciable considering that the polyplexe micelles have hydrophilic and neutral PEG palisades on their surface to shield the cationic character.

To verify that the improved transfection ability of the Lac-PEG-PSAO-PAMA/pDNA polyplex micelles is a result of the facilitated endosomal escape function as well as the enhanced cellular uptake through ASGP-mediated endocytosis, the transfection study at N/P = 3, 5, and 10 was carried out in the presence or the absence of hydroxychloroquine (HCQ) as an endosomolytic agent, nigericin (NR) (*38*) as an inhibitor of the

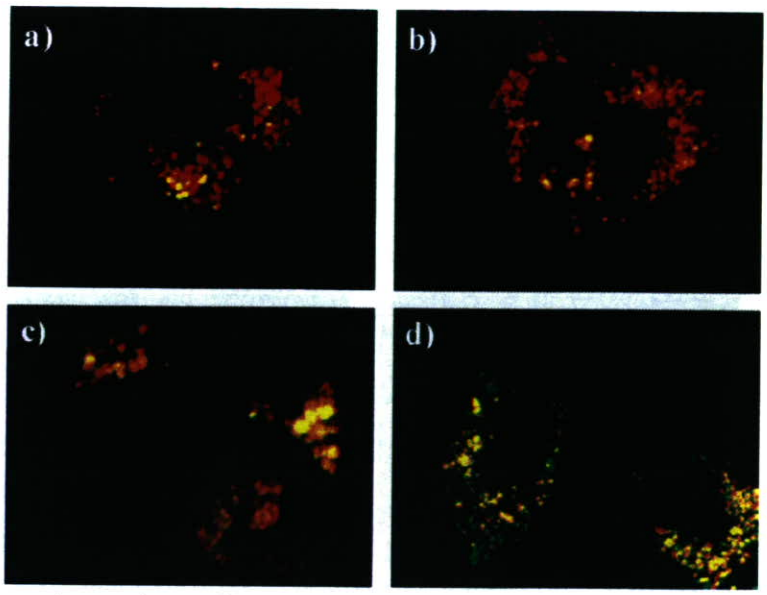

Figure 11. Confocal fluorescent microscope images of the HuH-7 cells in the presence of Lysotracker Red DND-99 and polyplex micelles prepared at N/P = 3 with FITC-labeled pDNA. (a) Lac-PEG-PAMA/pDNA polyplex micelles (incubation time: 30 min), (b) Lac-PEG-PAMA/pDNA polyplex micelles (incubation time: 120 min), (c) Lac-PEG-PSAO-PAMA/pDNA polyplex micelles, (incubation time: 30 min), (d) Lac-PEG-PSAO-PAMA/pDNA polyplex micelles (incubation time: 120 min). These images are the typical image of triplicate experiments.

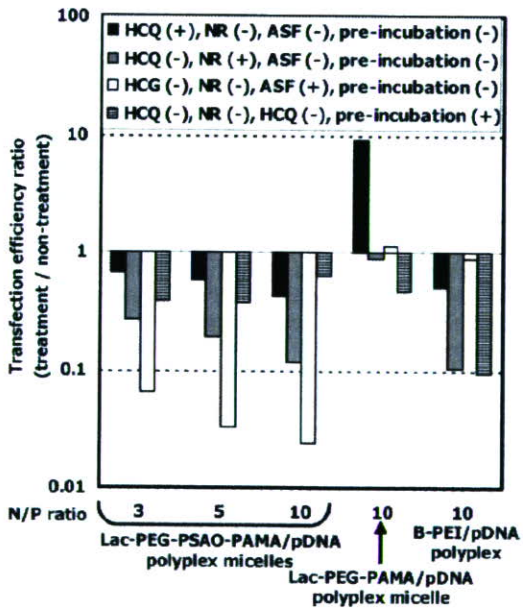

Figure 12. Effect of the HCQ (100 μM), NR (5 μM), ASF (4 mg/mL), and 20% serum preincubation on the transfection efficiency to HuH-7 cells of the Lac-PEG-PSAO-PAMA/pDNA polyplex micelle, Lac-PEG-PAMA/pDNA polyplex micelle, and B-PEI/pDNA polyplex as a function of N/P ratios at a fixed pDNA amount. Transfection efficiency ratio is described as [value of RLU/mg of protein treated with additive (HCQ, NR, and ASF)]/[value of RLU/mg of protein in Figure 11]. The plotted data are the average of triplicate experiments ± SD.

endosomal acidification, and ASF as an inhibitor of the ASGP-mediated endocytosis. As shown in Figure 12, HCQ treatment (100 μM) had no contribution in increasing the transfection efficiency for the Lac-PEG-PSAO-PAMA/pDNA polyplex micelles and the B-PEI/pDNA polyplex compared with the Lac-PEG-PAMA/pDNA polyplex micelle (about 1 order of magnitude increase in transfection efficiency), whereas it showed an appreciable decrease in the transfection efficiency in the presence of NR (5 μM) for the Lac-PEG-PSAO-PAMA/pDNA polyplex micelles and the B-PEI/pDNA polyplex. This is in line with the assumption that the Lac-PEG-PSAO-PAMA/pDNA polyplex micelles may be equipped with an endosome escaping function due to the unprotonated pH-responsive PSAO segment in the polyplex micelles.

A significant decrease in the transfection efficiency of the Lac-PEG-PSAO-PAMA/pDNA polyplex micelles was observed in the presence of ASF, consistent with the results of cellular uptake, as shown in Figure 9. Alternatively, no effect of ASF was observed even for the Lac-PEG-PAMA/pDNA polyplex micelle, suggesting that the endosomal escape may be the most critical barrier to intracellular gene delivery by Lac-PEG-PAMA/pDNA polyplex micelle. Thus, it may be reasonable to conclude that an appreciable fraction of the Lac-PEG-PSAO-PAMA/pDNA polyplex micelles is taken up into HuH-7 cells through the ASGP receptor-mediated endocytosis process mediated by the cluster of the large number of lactose moieties on the surface of the polyplex micelles, followed by the effective disruption of the endosome by the buffer effect of the unprotonated pH-responsive PSAO segment in the polyplex micelles.

It is well-known that components of the serum may interact with the polyplex to induce its structure change, resulting in decreasing transfection efficiency. Thus, we examined the effect of the 20% serum preincubation for 6 h on the transfection efficiency of Lac-PEG-PSAO-PAMA/pDNA, Lac-PEG-PAMA/pDNA polyplex micelles, and B-PEI/pDNA polyplexes. As shown in Figure 12, 1 order of magnitude decrease in the transfection efficiency was observed for B-PEI/pDNA polyplexes after preincubation with 20% serum probably due to the nonspecific interaction of the cationic polyplexes with negatively charged biomacromolecules, inducing the decrease in the cellular uptake. In a sharp contrast, the polyplex micelle sytems still retained sufficient transfection efficiency toward HuH-7 cells even after preincubation with 20% serum. The almost neutral surface charge ($\zeta \sim +5$ mV in Table 1) of the Lac-PEG-PSAO-PAMA/pDNA polyplex micelles with the highly lactosylated PEG outer shell surrounding the PIC core and the PSAO inner shell may induce the micelles to tolerate serum components, allowing the cellular specific interaction through ASGP receptor-mediated endocytosis to retain efficiency even after the serum preincubation.

CONCLUSIONS

In conclusion, this study demonstrates the pH-responsive nature of novel three-layered polyplex micelles composed of a lactosylated-PEG-PSAO-PAMA triblock copolymer and pDNA, aimed at the development of a targetable and endosome-disruptive gene delivery system. The Lac-PEG-PSAO-PAMA triblock copolymer bearing a PAMA segment as the DNA-condensing polyamine and a PSAO segment as the pH-responsive polyamine was successfully synthesized. The Lac-PEG-PSAO-PAMA triblock copolymer, thus prepared, spontaneously associated with pDNA to form three-layered polyplex micelles with a PAMA/pDNA PIC core, a free PSAO inner shell, and a lactosylated PEG outer shell, as confirmed by ^{1}H NMR spectroscopy. Under physiological conditions, the Lac-PEG-PSAO-PAMA/pDNA polyplex micelles prepared at an N/P ratio above 3 were found to be able to condense pDNA (EtBr assay), thus forming polyplex micelles with a relatively small size (< 150 nm, DLS measurements), and an almost neutral surface charge ($\zeta \sim +5$ mV, zeta-potential measurements). The Lac-PEG-PSAO-PAMA/pDNA polyplex micelle formed at N/P = 3 exhibited a pH-induced size variation (pH = 7.4, 132.6 nm → pH = 4.0, 181.8 nm) corresponding to the conformational changes (globule-rod transition) in the uncomplexed PSAO chain in response to pH. The swelling of the free PSAO inner shell is likely to occur in this process while retaining the condensed PIC core composed of the PAMA segment and pDNA. The fluorescence microscopic observation revealed that the interaction of the polyplex micelle entrapping FITC-labeled pDNA with HuH-7 cells was significantly reduced in the presence of ASF compared to the condition without ASF, suggesting that ASGP receptor-mediated endocytosis would be a major route of the cellular uptake of the Lac-PEG-PSAO-PAMA/pDNA polyplex micelles. Furthermore, the Lac-PEG-PSAO-PAMA/pDNA polyplex micelles exhibited more efficient transfection ability than Lac-PEG-PSAO/pDNA and Lac-PEG-PAMA/pDNA polyplex micelles. Presumably, the Lac-PEG-PSAO-PAMA/pDNA polyplex micelles might have an endosomal escape function, and thus, hydroxychloroquine as an endosomolytic agent was not required to observe appreciable transfection. Several important factors are likely to be synergistically involved in the pronounced transfection efficiency of the Lac-PEG-PSAO-PAMA/pDNA polyplex micelles, such as minimal interaction with serum proteins, enhancement of the cellular uptake through ASGP receptor-mediated endocytosis, and effective transport to the cytoplasm from the endosomal compartment (endosomal escape). Therefore, the polyplex micelle composed of the ABC triblock copolymer, thus described here, would be a promising vector for smart gene delivery.

ACKNOWLEDGMENT

This work was supported by the Core Research for Evolutional Science and Technology (CREST) from the Japan Science and Technology Agency [JST]. We thank Professor Dr. Teiji Tsuruta for helpful comments on the preparation of the manuscript and Hiroshi Ogawa for the excellent experimental support.

Supporting Information Available: Other experimental procedures and results including synthesis of PEGs, the ^{1}H NMR spectrum of polyplex micelles at pD 4.0, and the MTT assay. This material is available free of charge via the Internet at http://pubs.acs.org.

LITERATURE CITED

(1) Yang, Y., Li, Q., Ertl, H. C., and Wilson, J. M. (1995) Cellular and humoral immune response to viral antigens create barrier to lung-directed gene therapy with recombinant adenoviruses. *J. Virol. 69*, 2004−2015.

(2) Yang, Y., Li, Q., Ertl, H. C., and Wilson, J. M. (1994) MHC class I-restricted cytotoxic T lymphocytes to viral antigens destroy hepatocytes in mice infected with E1-deleted recombinant adenoviruses. *Immunity 1*, 433−442.

(3) Gunter, K. C., Khan, A. S., and Noguchi, P. D. (1993) The safety of retroviral vectors. *Hum. Gene Ther. 4*, 643−645.

(4) Wakebayashi, D., Nishiyama, N., Itaka, K., Miyata, K., Yamasaki, Y., Harada, A., Koyama, H., Nagasaki, Y., and Kataoka, K. (2004) Polyion complex micelles of pDNA with acetal-poly(ethylene glycol)-poly(2-(dimethylamino)ethyl methacrylate) block copolymer as the gene carrier system: physicochemical properties of micelles relevant to gene transfection efficacy. *Biomacromolecules 5*, 2128−2136.

(5) Itaka, K., Yamauchi, K., Harada, A., Nakamura, K., Kawaguchi, H., and Kataoka, K. (2003) Polyion complex micelles from plasmid DNA and poly(ethylene glycol)-poly(L-lysine) block copolymer as serum-tolerable polyplex system: physicochemical properties of micelles relevant to gene transfection efficiency. *Biomaterials 24*, 4495−4506.

(6) Itaka, K., Yamauchi, K., Harada, A., Nakamura, K., Kawaguchi, H., and Kataoka, K. (2002) Evaluation by fluorescence resonance energy transfer of the stability of nonviral gene delivery vectors under physiological conditions. *Biomacromolecules 3*, 841−845.

(7) Harada-Shiba, M., Yamauchi, K., Harada, A., Takamisawa, I., Shimokado, K., and Kataoka, K. (2002) Polyion complex micelles as vectors in gene therapy-pharmacokinetics and in vivo gene transfer. *Gene Therapy 9*, 407−417.

(8) Kataoka, K., Harada, A., Wakebayashi, D., and Nagasaki, Y. (1999) Polyion complex micelles with reactive aldehyde groups on their surface from plasmid DNA and end-functionalized charged block copolymers. *Macromolecules 32*, 6892−6894.

(9) Katayose, K., and Kataoka, K. (1998) Remarkable increase in nuclease resistance of plasmid DNA through supramolecular assembly with poly(ethylene glycol)-poly(L-lysine) block copolymer. *J. Pharm. Sci. 87*, 160−163.

(10) Katayose, S., and Kataoka, K. (1997) Water-soluble polyion complex associates of DNA and poly(ethylene glycol)-poly(L-lysine) block copolymer. *Bioconjugate Chem. 8*, 702−707.

(11) Wakebayashi, D., Nishiyama, N., Yamasaki, Y., Itaka, K., Kanayama, N., Harada, A., Nagasaki, Y., and Kataoka, K. (2004) Lactose-conjugated polyion complex micelles incorporating plasmid DNA as a targetable gene vector system: their preparation and gene transfecting efficiency against cultured HepG2 cells. *J. Control. Release 95*, 653−664.

(12) van de Wetering, P., Cherng, J. Y., Talsma, H., Crommelin, D. J. A., and Hennink, W. E. (1998) 2-(Dimethylamino)ethyl methacrylate based (co)polymers as gene transfer agents. *J. Control. Release 53*, 145−153.

(13) Cherng, J. Y., Van de Wetering, P., Tslsma, H.; Crommelin, D. J. A., and Hennink, W. E. (1996) Effect of size and serum proteins on transfection efficiency of poly ((2-dimethylamino)ethyl methacrylate)-plasmid nanoparticles. *Pharm. Res. 13*, 1038−1042.

(14) Brown, M. D., Schatslein, A. G., and Uchegbu, I. F. (2001) Gene delivery with synthetic (non viral) carriers. *Int. J. Pharm. 229*, 1−21.

(15) Nishikawa, M., and Huang, L. (2001) Nonviral vectors in the new millennium: delivery barriers in gene transfer. *Hum. Gene Ther. 12*, 861−870.

(16) Lloyd, J. B. (2000) Lysosome membrane permeability: implications for drug delivery. *Adv. Drug Deliv. Rev. 41*, 189−200.

(17) Gruenberg, J. (2001) The endocytic pathway: a mosaic of domains. *Nat. Rev.: Mol. Cell. Biol. 2*, 721−730.

(18) Clague, M. J. (1998) Molecular aspects of the endocytic pathway. *Biochem. J. 336*, 271−282.

(19) Mukherjee, S., Ghosh, R. N., and Maxfield, F. R. (1997) Endocytosis. *Physiol. Rev. 77*, 759−803.

(20) Duncan, R. (1992) Drug-polymer conjugates: potential for improved chemotherapy. *Anti-Cancer Drugs 3*, 175−210.

(21) Boussif, O., Lezoualc, F., Zanta, M. A., Mergny, M. D., Scherman, D., Demeneix, B., and Behr, J. P. (1995) A versatile vector for gene

and oligonucleotide transfer into cells in culture and in vivo: polyethylenimine. *Proc. Natl. Acd. Sci. U.S.A. 92*, 7297−7301.
(22) Kabanov, A. V., Bronich, T. K., Kabanov, V. A., Yu, K., and Eisenberg, A. (1998) Soluble stoichiometric complexes from poly(*N*-ethyl-4-vinylpyridinium) cations and poly(ethylene oxide)-*block*-polymethacrylate anions. *Macromolecules 29*, 6797−6802.
(23) Fukushima, S., Miyata, K., Nishiyama, N., Kanayama, N., Yamasaki, Y., and Kataoka, K. (2005) PEGylated polyplex micelles from triblock catiomers with spatially ordered layering of condensed pDNA and buffering units for enhanced intracellular gene delivery. *J. Am. Chem. Soc. 127*, 2810−2811.
(24) Nagasaki, Y., Luo, L. B., Tsuruta, T., and Kataoka, K. (2001) Novel pH-sensitive poly(silamine) hydrogel microsphere possessing a stable skin layer. *Macromol. Rapid Commun. 22*, 1124−1127.
(25) Luo, L. B., Kato, M., Tsuruta, T., Kataoka, K., and Nagasaki, Y. (2000) Stimuli-sensitive polymer gels that stiffen upon swelling. *Macromolecules 33*, 4992−4994.
(26) Nagasaki, Y., Kazama, K., Honzawa, E., Kato, M., Kataoka, K., and Tsuruta, T. (1996) A hydrogel with rubber elasticity transition. *Macromol. Symp. 109*, 27−40.
(27) Nagasaki, Y., Kazama, K., Honzawa, E., Kato, M., Kataoka, K., and Tsuruta, T. (1995) Rubber elasticity transition of poly(silamine) induced by ionic interactions. *Macromolecules 28*, 8870−8871.
(28) Nagasaki, Y., Honzawa, E., Kato, M., and Kataoka, K. (1994) Novel stimuli-sensitive telechelic oligomers. pH and temperature sensitivities of poly(silamine) oligomers. *Macromolecules 27*, 4848−4850.
(29) Nagasaki, Y., Honzawa, E., Kato, M., Kihara, Y., and Tsuruta, T. (1992) Novel synthesis of a macromonomer having organosilyl and amino groups. *J. Macromol. Sci., Pure Appl. Chem. A29*, 457−470.
(30) van de Wetering, P., Schuurmans-Nieuwenbroek, N. M. E., Hennink, W. E., and Storm. G. (1999) Comparative transfection studies of human ovarian carcinoma cells in vitro, ex vivo and in vivo with poly(2-(dimethylamino)ethyl methacrylate)-based polyplexes. *J. Gene Med. 1*, 156−165.
(31) Cherng, J. Y., Talsma, H., Verrijik, R., Crommelin, D. J., and Hennink, W. E. (1999) The effect of formulation parameters on the size of poly-((2-dimethylamino)ethyl methacrylate)-plasmid complexes. *Eur. J. Pharm. Biopharm. 47*, 215−224.
(32) Nagasaki, Y., Sato, Y., and Kato, M. (1997) A novel synthesis of ssemitelechelic functional poly(methacrylate)s through an alcoholate-initiated polymerization. Synthesis of poly[2-(N,N-diethylaminoethyl) methacrylate] macromonomer. *Macromol. Rapid Commun. 18*, 827−835.
(33) Kitano, H., Shoda, K., and Kosaka, A. (1995) Galactose-containing amphiphiles prepared with a lipophilic radical initiator. *Bioconjugate Chem. 6*, 131−134.
(34) Hashida, M., Takemura, S., Nishikawa, M., and Takakura, Y. (1998) Targeted delivery of plasmid DNA complexed with galactosylated poly(L-lysine). *J. Controlled Release 53*, 301−310.
(35) Stockert, R. J. (1995) The asialoglycoprotein receptor: relationships between structure, function, and expression. *Physiol. Rev. 75*, 591−609.
(36) Zanta, M. A., Boussif, O., Adib, A., and Behr, J. P. (1997) In vitro gene delivery to hepatocytes with galactosylated polyethylenimine. *Bioconjugate Chem. 8*, 839−844.
(37) Plank, C., Mechter, K., Szoka, F. C., Jr., and Wagner, E. (1996) Activation of the complement system by synthetic DNA complexes: a potential barrier for intravenous gene delivery. *Hum. Gene Ther. 7*, 1437−1446.
(38) Uherek, C., Fominaya, J., and Wels, W. (1998) A modular DNA carrier protein based on the structure of diphtheria toxin mediates target cell-specific gene delivery. *J. Biol. Chem. 273*, 8835−8841.

BC050364M

THE JOURNAL OF BIOLOGICAL CHEMISTRY VOL. 281, NO. 37, pp. 27229–27241, September 15, 2006

Pro-inflammatory Cytokine Tumor Necrosis Factor-α Induces Bone Morphogenetic Protein-2 in Chondrocytes via mRNA Stabilization and Transcriptional Up-regulation*

Received for publication, April 10, 2006, and in revised form, June 12, 2006 Published, JBC Papers in Press, July 11, 2006, DOI 10.1074/jbc.M603385200

Naoshi Fukui[‡1], Yasuko Ikeda[‡], Toshiyuki Ohnuki[‡], Atsuhiko Hikita[‡], Sakae Tanaka[§], Shoji Yamane[‡], Ryuji Suzuki[‡], Linda J. Sandell[¶], and Takahiro Ochi[‡]

From the [‡]Department of Pathomechanisms, Clinical Research Center, National Hospital Organization Sagamihara Hospital, Sagamihara, Kanagawa 228-8522, Japan, the [§]Department of Orthopaedic Surgery, Faculty of Medicine, the University of Tokyo, Bunkyo-ku, Tokyo 113-0033, Japan, and the [¶]Department of Orthopaedic Surgery, Washington University School of Medicine, St. Louis, Missouri 63110

In articular chondrocytes, the inflammatory cytokine tumor necrosis factor-α (TNF-α) induces the expression of bone morphogenetic protein-2 (BMP-2), a growth factor known to be involved in the induction of cartilage and bone. A study was performed to clarify the mechanism(s) underlying the induction of BMP-2 in chondrogenic ATDC5 cells and primary cultured adult human articular chondrocytes. In ATDC5 cells, the endogenous BMP-2 expression was consistently low throughout the process of chondrogenic differentiation, and TNF-α induced BMP-2 expression only after the cells acquired the chondrogenic phenotype. The results of nuclear run-off assay and cycloheximide treatment consistently indicated that ATDC5 cells acquire the capacity to synthesize BMP-2 mRNA in the nuclei during the differentiation process. In an attempt to explain the discrepancy between the active nuclear mRNA synthesis and the observed low expression level in differentiated ATDC5 cells, the stability of BMP-2 mRNA was evaluated, and the cells were found to regulate the expression of BMP-2 at the post-transcriptional level. Human chondrocytes were confirmed to have a similar post-transcriptional regulation. The result of 3′-rapid amplification of cDNA end revealed that both human and mouse BMP-2 mRNAs contain multiple pentameric AUUUA motifs in a conserved manner in the 3′-untranslated regions, and transient transfection experiments demonstrated that TNF-α increases the stability of BMP-2 mRNA through the pentameric motifs. Further experiments revealed that TNF-α modulates mRNA stability via p38 signal transduction pathway, whereas the cytokine also augmented the expression of BMP-2 through transcriptional up-regulation via the transcriptional factor NF-κB.

Bone morphogenetic proteins (BMPs)[2] are a group of secreted signaling proteins that were originally identified by their ability to induce ectopic bone formation (1). Molecular cloning of the BMPs later revealed that the proteins belong to the transforming growth factor-β superfamily (2). The evolutionary conservation of BMPs is remarkable. For example, the amino acid sequence of *Drosophila* protein *decapentaplegic* (*dpp*) is ~75% identical to human BMP-2 and is functionally interchangeable with recombinant human protein as to its ability to ectopically induce bone formation in rodents (3).

BMPs are critical in embryonal development and postnatal growth. Among them, BMP-2 plays a vital role in fetal development. Mice lacking functional BMP-2 gene die during early embryogenesis due to malformation of the proamniotic canal and a defect in cardiac development (4). Subsequent studies have shown that the growth factor is involved in various aspects of development such as skin and hair formation, neural cell differentiation, and cartilage and bone formation (5). The role of BMP-2 in skeletal development is particularly crucial. At the early stage of embryogenesis, BMP-2 is expressed in specific areas of limb buds to form prechondrogenic condensations, and it later promotes cellular differentiation into chondrocytes (6).

Besides its roles in developmental and growth processes, BMP-2 is also expressed in postnatal animals and is often associated with various pathologies. The growth factor is expressed in the process of bone healing where it regulates cellular differentiation, proliferation, and matrix production (7, 8). Various tumors have been found to express BMP-2. Indeed, this protein is known to exert diverse effects on tumor cells, ranging from the facilitation of tumor growth to the induction of cellular apoptosis (9–11). We and other investigators have found that BMP-2 is expressed at high levels in arthritic joints by both chondrocytes and synovial cells, possibly promoting chondrocyte anabolism and osteophyte formation (12–16).

Because of its potent biological actions, the expression of BMP-2 must be strictly regulated *in vivo*. In fact, BMP-2 is expressed in a highly tissue- and stage-specific pattern during embryogenesis (17, 18), and either enhancement or inhibition

* This work was supported in part by Grants-in-aid from the Japan Society for the Promotion of Science (Grant 15390467), the Ministry of Education, Culture, Sports, Science and Technology of Japan (Grant 16659416), the Mitsui Life Social Welfare Foundation, the Nakatomi Foundation. The costs of publication of this article were defrayed in part by the payment of page charges. This article must therefore be hereby marked "*advertisement*" in accordance with 18 U.S.C. Section 1734 solely to indicate this fact.

[1] To whom correspondence should be addressed. Tel.: 81-42-742-8311; Fax: 81-42-742-7990; E-mail: n-fukui@sagamihara-hosp.gr.jp.

[2] The abbreviations used are: BMP, bone morphogenetic protein; UTR, untranslated region; TNF, tumor necrosis factor; GAPDH, glyceroaldehyde-3-phsophate dehydrogenase; ARE, AU-rich element; nt, nucleotide; NF-κB, nuclear factor-κB; IκBα, inhibitor of κBα; PDTC, pyrrolidine dithiocarbamate; MAP, mitogen-activated protein; MKK, mitogen-activated protein kinase kinase; CHX, cycloheximide; ActD, actinomycin D; ERK, extracellular signal-regulated kinase; JNK, c-Jun N-terminal kinase; RNAi, RNA interference; siRNA, small interfering RNA.

of its activity is know to cause a significant disturbance in skeletal formation (19, 20). However, although the function of BMP-2 has been extensively studied, less is known about the mechanisms that regulate production of the growth factor. To date, several studies have shown that the expression of the gene is regulated at the transcriptional level. Retinoic acid induces BMP-2 expression through transcriptional activation in osteoblastic cells, possibly via retinoic acid receptor γ (21–23). NF-κB has been shown to regulate the transcriptional activity of BMP-2 in growth plate chondrocytes during endochondral bone development (24). The transcriptional activity might be enhanced by estrogen (25) and, interestingly, by BMP-2 itself (26). Thus, transcriptional regulation is considered to play an important role in expression of the protein.

On the other hand, BMP-2 expression could also be regulated at the post-transcriptional level. Computer analyses have revealed that the proximal part of the 3′-untranslated region (3′-UTR) of BMP-2 gene is highly conserved across a wide range of species (21, 27). That fact suggests the involvement of post-transcriptional regulation for the expression of BMP-2, because 3′-UTRs of mRNA often contain sequences to regulate post-transcriptional events (28, 29). In fact, a recent report has shown that degradation of the gene transcripts could be regulated by the region (27). However, details of the regulatory mechanism are not yet known, and the biological significance of transcriptional and post-transcriptional regulation has yet to be established.

We and others recently reported that the pro-inflammatory cytokines interleukin-1β and TNF-α induce BMP-2 expression in adult articular chondrocytes and a chondrosarcoma cell line (12, 30). Similar BMP-2 induction by those cytokines is also observed in synovial cells (14, 31) and could be a widespread event in arthritic joints. In this study, the mechanism of BMP-2 induction by TNF-α was studied in chondrogenic ATDC5 cells and primary cultured adult human articular chondrocytes. Our results indicated that both transcriptional and post-transcriptional regulation are involved in the induction of BMP-2.

EXPERIMENTAL PROCEDURES

Cell Culture—ATDC5 cells were obtained from the RIKEN cell bank (Tsukuba, Japan) and cultured in a 1:1 mixture of Dulbecco's modified Eagle's medium and Ham's F-12 medium (DMEM/F-12, Invitrogen) containing 5% fetal bovine serum (fetal bovine serum, Invitrogen), 50 units/ml penicillin, 50 μg/ml streptomycin, 10 μg/ml human transferrin (Roche Molecular Biochemicals, Indianapolis, IN), and 3×10^{-8} M sodium selenite (Sigma) (32). To induce chondrogenic differentiation, bovine insulin (Sigma) was added to the media at a concentration of 10 μg/ml. Human chondrocytes were obtained from 29 osteoarthritic knee joints in 28 patients at the time of joint replacement surgery. The material collection was performed under the approval of institutional review boards, and informed consent in writing was obtained from all patients. Articular chondrocytes were liberated from cartilage tissue by sequential enzymic digestion of 0.5% Pronase (Calbiochem) and 0.025% collagenase P (Roche Diagnostics, Basel, Switzerland) (33). Isolated cells were plated onto 6- or 12-well plates at a density of 2×10^5 cells/cm^2 and cultured in DMEM/F-12 media containing 10% fetal bovine serum, penicillin, streptomycin, and 25 μg/ml ascorbic acid (Sigma). For cartilage explants, full thickness articular cartilage was aseptically obtained from metacarpophalangeal joints of adult bovine animals and punched out into discs 3 mm in diameter. The explants were cultured in DMEM (Invitrogen) containing 10% fetal bovine serum, penicillin, streptomycin, and 25 μg/ml ascorbic acid.

For the inhibitors used in the study, cycloheximide, actinomycin D, pyrrolidine dithiocarbamate, ionomycin, and wortmannin were purchased from Sigma, U0126 and SP600125 were from Biomol (Plymouth Meeting, PA), and SB202190, SB202474, SB203580, PD98059, and GF109203X were obtained from Calbiochem. Recombinant mouse and human TNF-α were purchased from Chemicon International (Temecula, CA); recombinant mouse noggin was from R&D Systems (Minneapolis, MN).

Real-time Quantitative PCR Analysis—Total RNA was extracted from the cells using the RNeasy kit (Qiagen, Valencia, CA) with DNaseI (Qiagen) treatment, and 1 μg of total RNA was employed to synthesize cDNA using avian myeloblastosis virus reverse transcriptase (Roche Diagnostics). The cDNA was then used for real-time quantitative PCR on a LightCycler (Roche Diagnostics). For mouse BMP-2 and glyceraldehyde-3-phosphate dehydrogenase (GAPDH) genes, respective pairs of gene-specific hybridization probes labeled with fluorescein (Flu) and LightCycler-Red640 (LC640) dyes, respectively, were used to monitor the amount of PCR product. The primer sequences were 5′-TGCACCAAGATGAACACAG-3′ and 5′-GCTGTTTGTGTTTGGCTTG-3′ for BMP-2, and 5′-TGAACGGGAAGCTCACTGG-3′ and 5′-TCCACCACCCTGTTGCTGTA-3′ for GAPDH. The probe sequences were 5′-TCGTTTGTGGAGCGGATGTCCTTTT/Flu/-3′ and 5′-/LC640/CATCATGTCCAAAAGTCACTAGCAATGGC-3′ for BMP-2, and 5′-CTGAGGACCAGGTTGTCTCCTGCGA/Flu/-3′ and 5′-/LC640/TTCAACAGCAACTCCCACTCTTCCACC-3′ for GAPDH (Nihon Gene Research Laboratory, Sendai, Japan). PCR of human BMP-2, RelA, Iκbα, and GAPDH genes was performed using the LightCycler FastStart DNA Master SYBR Green I (Roche Diagnostics), and the amount of PCR product was monitored by the intensity of fluorescence from the dye bound to the product. The primer sequences were 5′-CCCCGGGGTATCACGCCTTT-3′ and 5′-GCGACACCCACAACCCTCCA-3′ for BMP-2, 5′-CAGAGTTACCTACCAGGGCTATTC-3′ and 5′-TCTGACTCTGTGTCATAGCTCTCC-3′ for RelA, 5′-ACGAGCTTGTAGGAAAGGACTG-3′ and 5′-GCTGCTCTTCTATAGGAACTTGGA-3′ for IκBα, and 5′-CAGGGACTCCCCAGCAGT-3′ and 5′-GGCATTGCCCTCAACGACCA-3′ for GAPDH.

The PCR protocol was the same for all genes, *i.e.* 95 °C for 10 min to activate *Taq* polymerase, then 40 cycles of 95 °C for 10 s, 60 °C for 15 s, and 72 °C for 6 s. When SYBR green dye was used to monitor PCR, melting curves were routinely recorded to verify the singularity of the PCR product. In each sample, the level of cDNA was normalized by the expression of GAPDH.

Nuclear Run-off Assay—ATDC5 cells were seeded to 225-cm^2 flasks at a density of 2×10^3/cm^2 and incubated under the aforementioned conditions. Soon after reaching confluency or

following 15 days of culture in the insulin-containing media, the cells were incubated for another 48 h in the presence or absence of 20 ng/ml of recombinant mouse TNF-α. The cells were then harvested, lysed in 4 ml of the Nonidet P-40 buffer (10 mM Tris, pH 7.4, 10 mM NaCl, 3 mM $MgCl_2$, and 0.5% Nonidet P-40). The nuclei thus obtained were resuspended in glycerol storage buffer (40% glycerol, 50 mM Tris, pH 8.3, 5 mM $MgCl_2$, and 0.1 mM EDTA) and immediately stored in liquid nitrogen until use.

RNA transcripts were labeled by incubation of the nuclei in a reaction buffer (5 mM Tris, pH 8.0, 2.5 mM $MgCl_2$, 150 mM KCl, 0.5 mM ATP, 0.5 mM CTP, 0.5 mM GTP, and 1 mM dithiothreitol) containing 100 μCi of [α-^{32}P]UTP (10 mCi/ml, GE Healthcare, Piscataway, NJ) for 30 min at 30 °C. Nuclei from 1–3 × 10^8 cells were used for each transcript reaction. The reaction mixture was treated with DNase I and proteinase K, and RNA was isolated by phenol-chloroform extraction and ethanol precipitation. pCR2.1 vectors (Invitrogen) containing cDNAs for the entire mouse BMP-2 3′-UTR, partial mouse GAPDH, and full-length mouse β-actin were prepared respectively, together with an empty vector. Five micrograms of each plasmid was linearized by HindIII digestion, denatured with 0.2 M NaOH, blotted onto nylon membranes (Hybond-N, GE Healthcare), and immobilized by UV-cross-linking. The membrane was pre-hybridized with ULTRAhyb (Ambion, Austin, TX), and hybridization was then allowed to proceed at 42 °C for 14–16 h. The membranes were washed twice in 2 × SSC at 65 °C, treated with RNase A, and washed again in 2 × SSC at 37 °C. The analysis was performed by phosphorimaging using a Typhoon 9410 (GE Healthcare) with ImageQuaNT software (GE Healthcare).

3′-Rapid Amplification of cDNA Ends—The 3′-end of mouse BMP-2 gene was determined using a GeneRacer kit (Invitrogen) following the manufacturer's protocol. In brief, total RNA was extracted from bone tissues of C57BL/6 mice, and cDNA was synthesized using an oligo(dT)-adapter primer provided by the kit. The first PCR was performed using 1 μg of the synthesized cDNA as a template with mGSP1 (5′-AGAAAACGTCTCGCCACCCTCC-3′) and 3′ primer for the adaptor. The PCR product containing the 3′-end of human BMP-2 mRNA was obtained by using a nested PCR using the first PCR product as a template, and mGSP2 (5′-TACATTTGCCTGACACGCAGCA-3′) and the 3′-nested primer provided by the kit as primers. The PCR product was subcloned into pCR2.1 vector and subjected to DNA sequencing. The 3′-rapid amplification of cDNA ends of human BMP-2 mRNA was performed in the same manner, using total RNA from primary cultured chondrocytes to generate cDNA, and an external primer hGSP1 (5′-TGGCACGTCCGGGTTACCATGTTCATTA-3′) and an internal primer hGSP2 (5′-TGAAGCCCTTACAGGCCAAAGGACCACA-3′) for the first and nested PCR, respectively. DNA sequences were determined by using the Long-Read Tower System (GE Healthcare). Three clones were sequenced for each gene.

Plasmid Constructions—Luciferase reporter expression constructs harboring mouse BMP-2 3′-UTR at the 3′-end of the luciferase coding region were prepared in pcDNA3.1/Zeo(+) expression vector (Invitrogen). The luciferase cDNA was generated from pGL3-Basic vector (Promega) by PCR and cloned into the KpnI and EcoRI sites of pcDNA3.1/Zeo(+). cDNA for the entire 3′-UTR of mouse BMP-2 was generated by PCR and subcloned into pCR2.1 vector. Using the vector as a template, specific regions of the 3′-UTR were amplified by PCR and ligated into pcDNA3.1/Zeo(+) between the EcoRI and XbaI sites. Thus, either the entire or a specific region of mouse BMP-2 3′-UTR was placed between the luciferase gene and the BGH polyadenylation site of the vector. All constructs were analyzed by restriction mapping and DNA sequencing.

Transient Transfection Assays—Transient transfection experiments were performed in differentiated ATDC5 cells using each of the prepared luciferase vectors and a phRL-TK vector (Promega). The cells were plated on 12-well plates, and differentiation was induced as previously described. DNA transfection was carried out using the SuperFect transfection reagent (Qiagen). For each well, 0.5 μg of the luciferase vector and 1.5 μg of phRL-TK vector were mixed with 4 μl of SuperFect reagent and 75 μl of DMEM/F-12 medium, and the mixture was incubated for 10 min at room temperature. The reagent mixture was combined with 400 μl of the complete culture medium, which was transferred to the washed cell monolayer in each well. After incubation for 14–18 h, the medium containing transfection reagent was replaced with the complete medium. For some experiments, recombinant mouse TNF-α was added to the medium at a concentration of 10 ng/ml. The transfected cells were cultured for 48 h and then lysed in 100 μl of reporter lysis buffer (Promega). Luciferase activity was assayed on a luminometer (JNR AB-2100, Atto, Tokyo, Japan) using a Dual-Glo luciferase assay system (Promega). All transfection experiments were repeated at least three times in duplicate.

Preparation of Adenovirus Vector and Gene Transduction—The recombinant adenovirus vector carrying constitutively active MAP kinase kinase 6 (MKK6) gene under the control of chicken β-actin promoter and cytomegalovirus IE enhancer was generated by the DNA-terminal protein complex method (34). The adenovirus carrying β-galactosidase was obtained from BD Biosciences (San Jose, CA). Titers of the adenovirus were determined by an Adeno-X Rapid Titer kit (BD Biosciences) following the manufacturer's protocol. The titer was represented by the multiplicity of infection.

To infect the adenovirus vectors in cultured human chondrocytes, the culture media in each well of 6- or 12-well plates was replaced by 1.0 or 0.5 ml of serum-free DMEM/F-12 medium containing the adenoviruses at the indicated multiplicity of infection. The cells were incubated for 2 h under normal culture conditions, after which 5 times the volume of the complete medium was added to each well.

Western Blotting—Approximately 1 × 10^6 cells were lysed in 0.5 ml of radioimmune precipitation assay buffer containing proteinase inhibitors (0.5 ml of 50 mM Tris-HCl, pH 7.4, 150 mM NaCl, 1% (v/v) Triton X-100, 1% (w/v) sodium deoxycholate, 0.1% (w/v) SDS, and a mixture of proteinase inhibitors (Complete Mini, Roche Diagnostics)) for 10 min on ice with occasional mixing. The lysate was clarified by centrifugation at 12,000 × *g* for 20 min at 4 °C. Twenty micrograms of protein was subjected to SDS-PAGE with 8–16% polyacrylamide sepa-

rating gel in the reducing condition and electronically transferred onto a nitrocellulose membrane (Bio-Rad). After blocking, the membrane was incubated with either anti-p38 MAP kinase or anti-phopho-p38 MAP kinase (Thr-180/Thy-182) antibody (Cell Signaling Technology, Beverly, MA) and then with the secondary antibody conjugated with peroxidase (Santa Cruz Biotechnology, Santa Cruz, CA). Immunoreactive protein was finally visualized using a SuperSignal West Pico chemiluminescent substrate (Pierce).

RNAi Experiments—The expression of p65 subunit of NF-κB or RelA and IκBα was suppressed by RNAi in primary cultured human chondrocytes. All siRNAs were purchased from Qiagen, and two siRNAs with distinctive sequences were used for each gene. The sense strand sequences of the RNA duplexes were as follows: RelA#1, 5′-GGACAUAUGAGACCUUCAAdTdT-3′; RelA#2, 5′-GAUUGAGGAGAAACGUAAAdTdT-3′; IκBα#1, 5′-GGGUGUACUUAUAUCCACATdT-3′; IκBα#2, 5′-GGGCCAGCUGACACUAGAAdTdT-3′; and control siRNA, 5′-UUCUCCGAACGUGUCACGUdTdT-3′.

The siRNAs were delivered into human chondrocytes by electroporation following cell isolation from cartilage matrix. Electroporation was performed using a Nucleofector® device and a Human Chondrocyte Nucleofector kit (Amaxa, Cologne, Germany) following the manufacturer's instructions. In brief, 1×10^6 cells were suspended in 100 μl of the electroporation buffer provided by the kit, along with 1.5 μl of 68 μM stock solution of siRNA. Thus, the final concentration of siRNA in the buffer was ~100 nM. The buffer was then transferred to a supplied cuvette, and electroporation was performed using the protocol recommended by the manufacturer. After electroporation, the cells were immediately transferred onto each well of 12-well plates and cultured in DMEM/F-12 containing 20% fetal bovine serum. Next day, the media were replaced to the aforementioned regular culture media for human chondrocytes. The viability of cells was ~60% with the procedure.

Incorporation of [^{35}S]Sulfate into Cartilage Explants—For this experiment, 20–40 cartilage explants were prepared from normal bovine articular cartilage and equally divided into 4 groups. The first group was cultured in the aforementioned culture medium for 6 days, while changing the medium every 2 days. The second group was first cultured in the same medium for 4 days, and then for 2 days in a medium containing recombinant mouse noggin (1 μg/ml). The third and fourth groups were initially cultured in a medium containing 2.5 ng/ml recombinant human TNF-α for 4 days. The third group was then cultured in the regular culture medium for 2 days, whereas the fourth group was cultured in a medium containing 1 μg/ml recombinant noggin. For all four groups, newly synthesized sulfated proteoglycan was radiolabeled for the last 8 h of culture with 10 μCi/ml [^{35}S]sulfate (GE Healthcare). The explants were then recovered, extensively rinsed with ice-cold phosphate-buffered saline, and subjected to papain digestion. The digestion was performed using 50 μg/ml papain (Sigma) in 500 μl of digestion buffer (0.2 M sodium acetate, pH 6.0) at 60 °C overnight. The digest was then centrifuged, and 20 μl of supernatant was used to measure the radioactivity. DNA content was also determined using a PicoGreen® double-stranded DNA quantitation kit (Invitrogen), and the radioactivity was normalized by the amount of DNA.

Immunohistochemistry—Immunohistochemistry of cartilage explants was performed following a previously described method (12) with some modifications. In brief, 6-μm-thick cryosections were prepared from the explants, fixed in acetone, and digested with 1.0% hyaluronidase (Sigma) for antigen retrieval. To detect the presence of BMP-2, anti-human BMP-2 goat polyclonal antisera (Santa Cruz Biotechnology) were used at the concentration of 1:100, which was visualized with the avidine-linked peroxidase system (goat ABC staining system, Santa Cruz Biotechnology) coupled with 3-amino-9-ethylcarbazole substrate (DakoCytomation, Carpinteria, CA). The sections were observed under a light microscope without nuclei staining, to facilitate direct comparison of the staining intensities among the sections.

Statistical Analyses—For statistical analyses, data were compared using one-way factorial analysis of variance, and when necessary, Fisher's PLSD was used as a post-hoc test. Statistical significance was set at $p < 0.05$.

RESULTS

TNF-α and Cycloheximide Induced BMP-2 Expression in Differentiated, Not Undifferentiated, ATDC5 Cells—As a preliminary experiment, the time course of chondrogenic differentiation of ATDC5 cells was determined by evaluating the expression of type II procollagen and aggrecan as well as type X procollagen from Day 0 until Day 25, every 5 days after addition of insulin to the media. Under our experimental conditions, the expression of type II procollagen and aggrecan began to increase at Day 10 and rose continuously up to Day 25 (data not shown). Meanwhile, the expression level of type X procollagen was very low from Day 0 to Day 15 and then was up-regulated at Day 20 and beyond (data not shown), indicating the occurrence of a hypertrophic change in the cells. Based on these observations, the induction of BMP-2 by TNF-α in ATDC5 cells was investigated between Days 0 and 15 in the following experiments.

Without TNF-α stimulation, the expression level of BMP-2 was consistently low in ATDC5 cells from Day 0 to Day 15 (Fig. 1, *A–D*). The response to TNF-α varied according to the stage of chondrogenic differentiation. At Days 0 and 5 when the cells were still undifferentiated, TNF-α did not induce the expression of BMP-2. With the onset of chondrogenic differentiation, a weak induction was observed at Day 10 (Fig. 1*C*), and it became obvious at Day 15 as the differentiation progressed (Fig. 1*D*). In Day-15 cells, the induction was dose-dependent, and its maximum was observed with 100 ng/ml TNF-α. The cells cultured for 15 days without insulin showed a weaker response to TNF-α, presumably due to the lack of chondrogenic differentiation (Fig. 1*E*).

Next, the effect of a protein synthesis inhibitor, cycloheximide (CHX), was studied at different stages of differentiation (Fig. 1*F*). In Day-0 cells, the expression of BMP-2 was not affected by CHX. In Day-10 cells, CHX induced a moderate expression of BMP-2, and in Day-15 cells the induction was obvious. In various genes, CHX is known to induce mRNA expression by disrupting the linkage between mRNA transla-

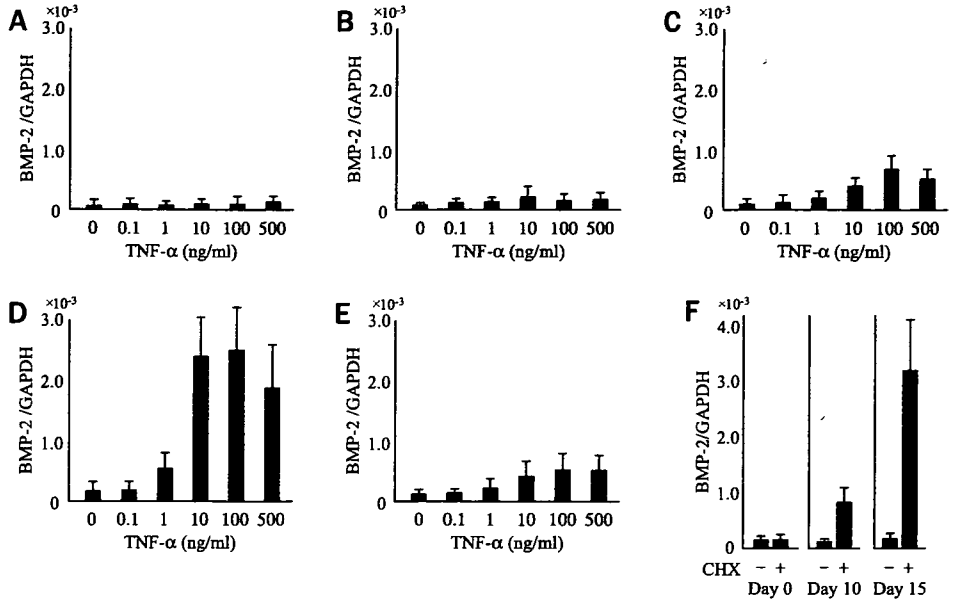

FIGURE 1. **Induction of BMP-2 in ATDC5 cells by TNF-α and cycloheximide.** *A–E*, effect of TNF-α on BMP-2 expression was evaluated on ATDC5 cells at various stages of chondrogenic differentiation. Before (*A*) and after culture for 5 (*B*), 10 (*C*), or 15 days (*D*) in insulin-containing media, ATDC5 cells were treated with graded doses of TNF-α for 48 h, and expression of BMP-2 mRNA was evaluated. In parallel, cells maintained for 15 days in insulin-free media were treated with TNF-α, and expression of BMP-2 was evaluated (*E*). *F*, ATDC5 cells cultured in insulin-containing media for 0, 10, or 15 days were treated with 2.5 μg/ml CHX for 24 h, and BMP-2 mRNA expression was evaluated. For these experiments, expression of BMP-2 mRNA was evaluated by real-time PCR together with GAPDH expression; results are shown in relative ratios against GAPDH. Data are mean ± S.D. of three to five experiments.

tion and mRNA degradation (35). Therefore, our result suggested the possibility that BMP-2 mRNA might have been synthesized at a certain level in differentiated ATDC5 cells, even though the observed expression level was very low.

BMP-2 Expression Is Regulated at Both Transcriptional and Post-transcriptional Levels in ATDC5 Cells—To determine the transcriptional activity of BMP-2 gene, a nuclear run-off assay was performed on differentiated and undifferentiated ATDC5 cells with or without TNF-α stimulation (Fig. 2, *A* and *B*). The result revealed that the expression of BMP-2 was suppressed at the transcriptional level in undifferentiated cells but that the gene transcripts were being synthesized at a substantial level in the nuclei of differentiated cells. In the differentiated ATDC5 cells, TNF-α treatment enhanced mRNA synthesis, whereas the cytokine had virtually no effect on it in undifferentiated cells.

Thus, results of the CHX treatment and nuclear run-off assay both indicated that, in ATDC5 cells, BMP-2 mRNA is synthesized at a certain level in the nuclei of cells once they acquired the chondrogenic phenotype. However, the observed level of BMP-2 expression was very low in the differentiated ATDC5 cells as long as they were not treated with TNF-α (Fig. 1, *A–D*). The apparent contradiction between the results strongly suggested the involvement of a post-transcriptional mechanism in the regulation of BMP-2 expression.

To examine this hypothesis, we evaluated the stability of BMP-2 mRNA in differentiated ATDC5 cells in the presence or absence of TNF-α. Because the basal expression level of BMP-2 was too low to evaluate the degradation rate, the cells were initially treated with TNF-α for 48 h to induce certain levels of BMP-2 expression, after which the degradation rate of mRNA was evaluated using an RNA synthesis inhibitor, actinomycin D (ActD). The result of this experiment revealed that the degradation rate of BMP-2 mRNA was indeed reduced by TNF-α (Fig. 2*C*). In the presence of TNF-α, the half-life of BMP-2 mRNA was extended from 137 to 257 min, an increase of ~88%. Thus, the involvement of a post-transcriptional mechanism in the induction of BMP-2 by TNF-α was indicated.

TNF-α Induces BMP-2 in Human Articular Chondrocytes by Increasing mRNA Stability—In the next experiment, the involvement of post-transcriptional mechanism(s) in the induction of BMP-2 was examined in primary cultured adult human articular chondrocytes. Before examining that hypothesis, the induction of BMP-2 in human chondrocytes was evaluated under our experimental conditions. The endogenous expression level of BMP-2 in human chondrocytes was considerably higher than that in differentiated ATDC5 cells, and, in accordance with our previous observation (12), TNF-α up-regulated BMP-2 expression ~10-fold (Fig. 3*A*). The induction was dose-dependent, and similar to that in ATDC5 cells, the maximum induction was observed at 100 ng/ml.

The experiment with CHX was repeated with human chondrocytes, and a strong induction of BMP-2 was again observed, suggesting the presence of a similar post-transcriptional regulation in human cells (Fig. 3*B*). The effect of CHX was observed at and above a concentration of 2.5 μg/ml, and 10 μg/ml CHX seemed sufficient to obtain the maximum induction.

Next, the stability of BMP-2 mRNA in human chondrocytes was evaluated in the presence or absence of TNF-α (Fig. 3*C*). Some cells were treated with TNF-α for 48 h, and the mRNA stability was then evaluated in the presence of TNF-α. The results showed that TNF-α also stabilizes BMP-2 mRNA in human articular chondrocytes. The mRNA half-life was extended ~2.6 times from 72 to 185 min by TNF-α. Interestingly, an extended TNF-α treatment for 48 h resulted in further mRNA stabilization, and the half-life was prolonged to 278 min, which was 390% of that in the untreated cells.

Human and Mouse BMP-2 mRNA Contain AU-rich Elements in 3′-UTRs—To determine the 3′-UTR sequence, 3′-rapid amplification of cDNA ends was performed on human and mouse BMP-2 mRNA. The results revealed that the 3′-UTR of human BMP-2 had a length of 3736 nt, whereas that of mouse 3′-UTR was 1170 nt (Fig. 4). Mouse 3′-UTR shows an 82% sequence identity with human 3′-UTR. Although both 3′-UTRs are longer than the average lengths of the respective species (29), they are both encoded by the third or the last exon of the gene together with the last part of the translated region.

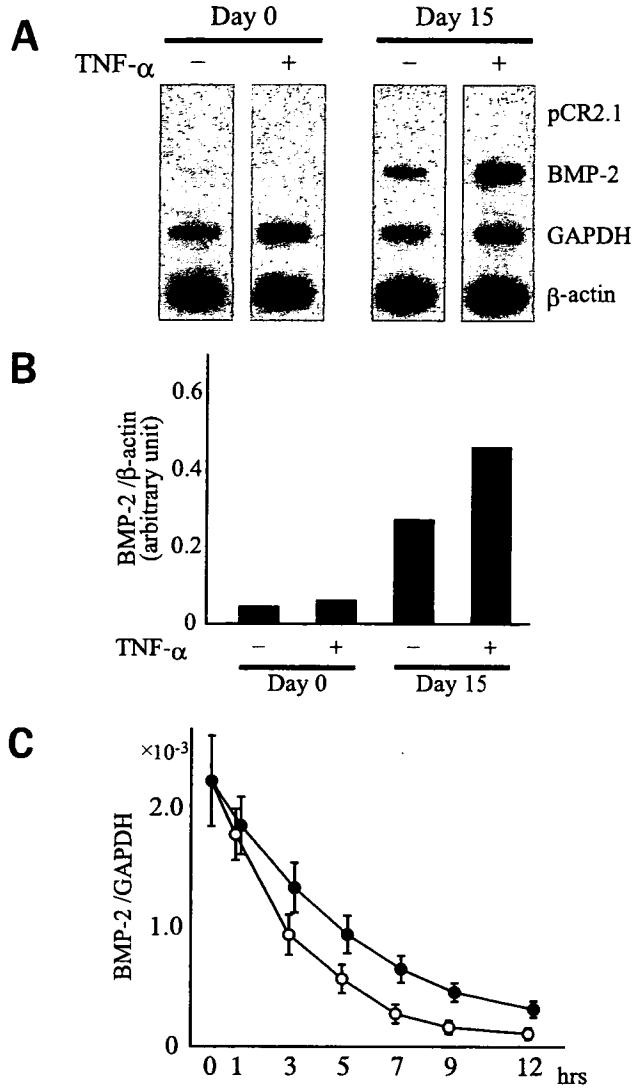

FIGURE 2. **Synthesis of BMP-2 mRNA in nuclei, and stability of mRNA in cytoplasm in the presence or absence of TNF-α.** *A*, nuclear run-offs from differentiated and undifferentiated ATDC5 cells. Immediately after reaching confluency (Day 0) or after culture in insulin-containing media for 15 days (Day 15), ATDC5 cells were treated with or without 20 ng/ml TNF-α for 48 h, and nuclei were obtained. RNA synthesis was allowed to proceed in nuclei in the presence of [α-^{32}P]UTP, and amounts of synthesized BMP-2 gene transcripts were evaluated by slot blot analysis together with those for GAPDH, β-actin, and pCR2.1 vector without insert (for background). The experiment was repeated twice with consistent results. *B*, signal ratios between BMP-2 3′-UTR and β-actin were quantified after subtracting background. *C*, ATDC5 cells were maintained in insulin-containing media for 15 days, and stimulated with 100 ng/ml TNF-α for 48 h to induce BMP-2 expression. Degradation of BMP-2 mRNA was then evaluated by addition of ActD (1 μM), with (*open circles*) or without (*filled circles*) withdrawal of TNF-α from media. At each time point, remaining amounts of BMP-2 mRNA were evaluated by real-time PCR together with GAPDH mRNA; results are shown in relative ratios against GAPDH. Data are mean ± S.D. of three experiments.

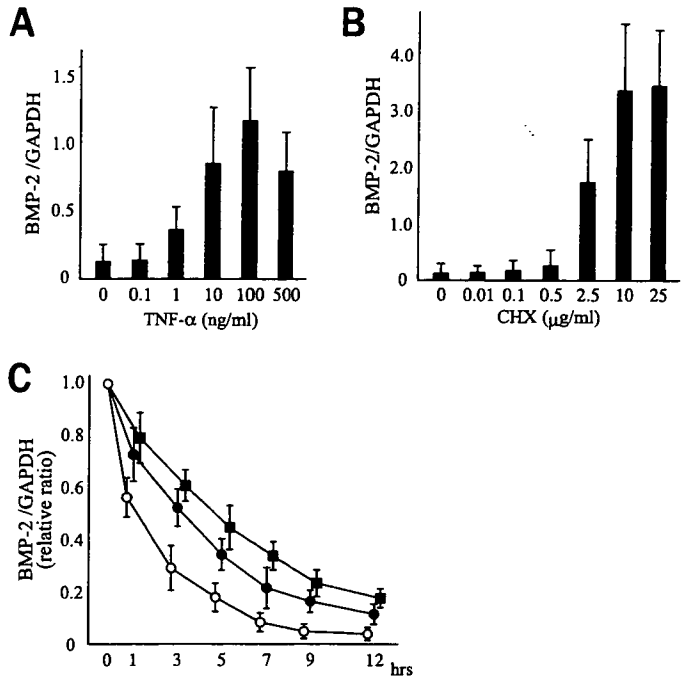

FIGURE 3. **Involvement of post-transcriptional regulation in expression of BMP-2 in human chondrocytes.** *A*, human articular chondrocytes were maintained by monolayer culture and treated with graded concentrations of TNF-α. Induction of BMP-2 was evaluated 48 h later. *B*, chondrocytes were treated with graded doses of CHX for 24 h, and BMP-2 expression was evaluated. *C*, decay of BMP-2 mRNA was evaluated in presence (*filled circles*) or absence (*open circles*) of TNF-α, using ActD (1 μM). Decay of mRNA was also evaluated in cells treated with TNF-α for 48 h prior to addition of ActD and in the continuous presence of the cytokine (*filled squares*). For these experiments, expression of BMP-2 was evaluated by real-time PCR together with GAPDH expression. In *A* and *B*, results are shown as ratios against GAPDH. In *C*, RNA ratios at respective time points were normalized by the ratio at beginning of the evaluation (*i.e.* time 0) in each experiment to facilitate direct comparison. Data are mean ± S.D. of three to five experiments.

For various genes, the stability of mRNA is regulated by cis-acting elements in 3′-UTR (28, 29). Among them, the adenosine/uridine-rich element (ARE) is a well characterized sequence that has the function of modulating mRNA degradation in response to various extracellular stimuli. The element often contains repeats of pentameric AUUUA motifs. The result of sequencing revealed that both human and mouse BMP-2 3′-UTRs contain multiple copies of the pentameric motif. Human 3′-UTR contains 22 motifs throughout the region, and mouse has 8 in the proximal third of the region (Fig. 4). The alignment of the 8 motifs in the mouse gene is well conserved in the human gene, suggesting their functional significance.

Induction of BMP-2 by TNF-α Is Mediated by the AU-rich Element in 3′-UTR—The functional significance of the ARE in BMP-2 3′-UTR was investigated by generating luciferase reporter constructs harboring either the entire or various parts of mouse BMP-2 3′-UTR at the 3′-end of the luciferase coding region (Fig. 5*A*).

To analyze the function of the region, that 3′-UTR was divided into four parts according to the distribution of pentameric AUUUA motifs. The first part, designated part A, involves the first 189 nt with two pentamers. The next 137 nt containing four pentamers was designated part B. Part C contained the following 114 nt with two pentamers, and the remaining 730 nt without motifs was designated part D. These parts were inserted, alone or in combination, after the stop codon of the luciferase coding region.

The constructs were transiently transfected to the differentiated ATDC5 cells, and the luciferase activity was measured (Fig. 5*B*). The results revealed that the addition of the entire 3′-UTR reduced luciferase activity by ~75%. When parts A, B, or D were inserted alone, a significant reduction was observed only with part B, whereas the reduction with parts A or D was

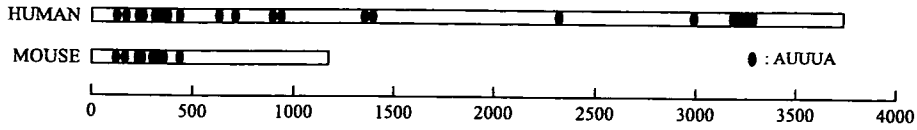

FIGURE 4. **Distribution of AUUUA motifs in human and mouse BMP-2 3′-UTRs.** Relative lengths and distributions of AUUUA motifs (*filled ellipses*) in human and mouse BMP-2 3′-UTRs are shown.

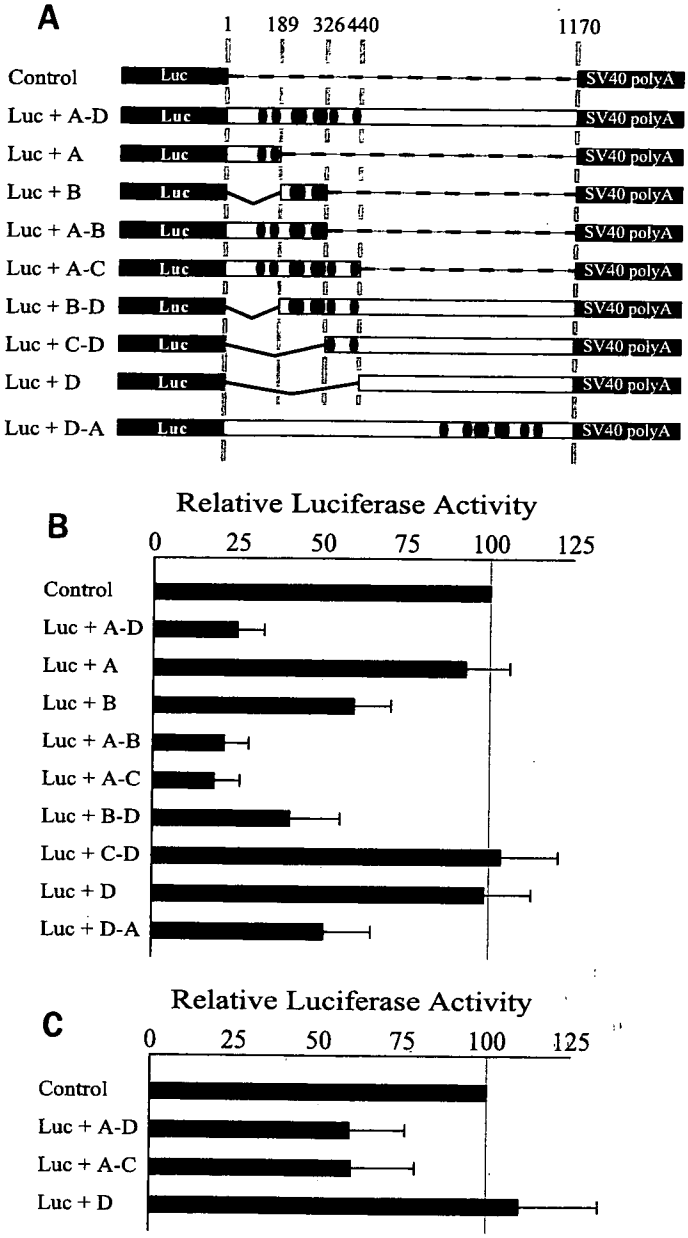

FIGURE 5. **Chimeric constructs used for transient transfection experiments and their luciferase activity.** *A*, chimeric constructs used for transient transfection experiments. Constructs have all or a part of mouse BMP-2 3′-UTR (*open bars*) at the 3′-end of luciferase coding sequence (*Luc*), followed by SV40 polyadenylation signal (*SV40 poly(A)*). The chimeric region was under the control of SV40 promoter and enhancer. *Solid ellipses* indicate locations of pentameric AUUUA motifs, and *numbers* at the *top* denote positions of nucleotide in 3′-UTR. *B*, luciferase activity of constructs. ATDC5 cells maintained for 15 days in insulin-containing media were transiently transfected with one of the above constructs, and luciferase activity was measured 48 h later. *C*, effect of TNF-α on luciferase activity. For some constructs, luciferase activity was measured after treating cells with 10 ng/ml TNF-α for 48 h following transfection. Luciferase assays were repeated three to six times, and activity of *Firefly* luciferase was normalized by that of *Renilla* luciferase. Data are expressed as a percentage of control (mean ± S.D.).

not apparent. The reduction of luciferase activity with part B was augmented by the addition of part A or parts C and D, and the strongest reduction was observed when parts A through C were inserted together. Interestingly, the addition of the reversed 3′-UTR sequence also suppressed luciferase activity, although the effect was less obvious than that of the regular orientation.

For some constructs, luciferase activity was also evaluated in the presence of TNF-α (Fig. 5*C*). For the two constructs that strongly reduced luciferase activity in the previous experiment, the suppressed activity was partly recovered by TNF-α, whereas the cytokine did not affect luciferase activity with the insert containing no AUUUA motifs. Thus, our results suggest the possibility that the expression of BMP-2 could have been suppressed in the chondrocytes by the ARE in 3′-UTR and that the induction of BMP-2 by TNF-α could have been the result of a release from the ARE-mediated suppression.

p38 Signaling Pathway Is Involved in Stabilization of BMP-2 mRNA by TNF-α in Human Chondrocytes—Next, experiments were performed to determine the signal transduction pathway(s) involved in the stabilization of BMP-2 mRNA by TNF-α. It is known that TNF-α stabilizes mRNA of various genes through the signal pathway involving p38 MAP kinase (36). For some other genes, the stability of mRNA is regulated by signal pathways involving extracellular signal-regulated kinase-1/2 (ERK-1/2) (37, 38), c-Jun N-terminal kinase (JNK) (39, 40), protein kinase C (38, 41), or phosphatidylinositol 3-kinase (42). mRNA turnover can be regulated by the intracellular calcium concentration (43). Thus, seven specific inhibitors for these signals were examined to determine whether they inhibited the induction of BMP-2 by TNF-α (Fig. 6*A*). Among them, SB203580, an inhibitor for p38 pathway, was found to strongly suppress the BMP-2 induction; it also suppressed the expression of BMP-2 in untreated chondrocytes by ~50%, suggesting that p38 signaling could be important in maintaining the endogenous expression of the protein. On the other hand, wortmannin and ionomycin, which inhibit phosphatidylinositol 3-kinase activity and cause calcium ion influx, respectively, induced the expression of BMP-2 in chondrocytes, although the induction by TNF-α was not enhanced but rather suppressed by these inhibitors. The inhibitors for ERK-1/2, JNK, or protein kinase C showed no significant effect on either the endogenous expression or induction levels, indicating that these pathways might not be involved in the regulation of BMP-2 expression in chondrocytes.

Because SB203580 showed significant suppression of BMP-2 expression, the dose response to the inhibitor was evaluated in the untreated and TNF-α-stimulated chondrocytes together with the effect of SB202190, another specific inhibitor for the p38 pathway (Fig. 6*B*). The result showed that the endogenous expression and induction of BMP-2 was inhibited by SB203580 in a similar dose-dependent manner. The endogenous expression and induction were both reduced by ~25% with 1 μM SB203580, and the inhibitory effects were almost maximal at the concentration of 5 μM.

The expression of BMP-2 was inhibited by SB202190 to an extent similar to SB203580 in both untreated and TNF-α stimulated chondrocytes, confirming the significance of p38 signaling in the maintenance of endogenous expression and induction of the protein by TNF-α.

We then evaluated the effect of SB203580 on the stability of BMP-2 mRNA in the TNF-α-treated chondrocytes and untreated cells (Fig. 6*C*). Even without TNF-α stimulation, the inhibition of the p38 pathway resulted in the facilitation of mRNA degradation in chondrocytes; the half-life of BMP-2 mRNA declined from 70 to 42 min, a reduction of ~40%. The decrease in mRNA stability was considered to account for the suppression of endogenous BMP-2 expression by the inhibitor. Furthermore, although the mRNA stability was significantly

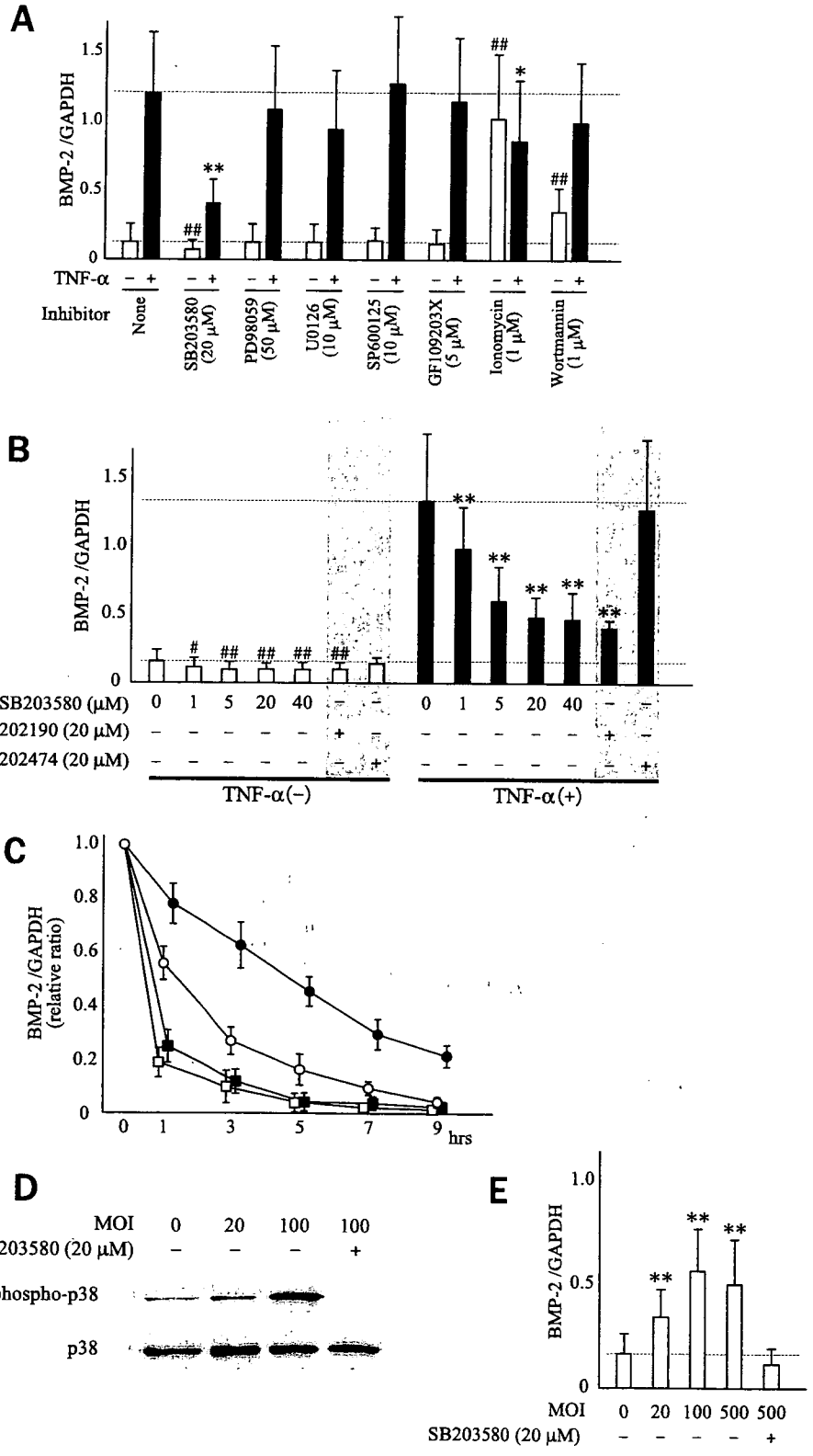

increased in the TNF-α-treated cells, the inhibitor reduced the stability below the level of that in untreated cells, completely abrogating the cytokine's effect. The mRNA half-life was 282 min in the TNF-α-treated cells, which was reduced to 53 min by the addition of SB203580.

The significance of p38 MAP kinase in the regulation of BMP-2 expression was confirmed by use of the adenovirus carrying constitutively active MKK6, a kinase that directly phosphorylates p38 MAP kinase. Infection with the adenovirus induced the expression of BMP-2 mRNA along with the phosphorylation of p38 (Fig. 6, *D* and *E*), but that induction was completely inhibited by SB203580, together with p38 phosphorylation. Thus, the results of these experiments showed that BMP-2 expression in primary cultured adult human chondrocytes is regulated by a post-transcriptional mechanism predominantly modulated by the p38 signal pathway.

Coordination of NF-κB and p38 Signal Pathway in BMP-2 Induction by TNF-α—Since it has been reported that the expression of BMP-2 is transcriptionally regulated by NF-κB in epiphyseal chondrocytes (24), experiments were performed to determine the role of NF-κB in the induction of BMP-2 by TNF-α. In the first experiment, nuclear translocation of NF-κB was inhibited by pyrrolidine dithiocarbamate (PDTC), and the levels of endogenous expression and induction by TNF-α were evaluated (Fig. 7*A*). Unlike SB203580, PDTC did not change the endogenous level of BMP-2 expression in human chondrocytes, suggesting that the transcriptional factor may not be responsible for the maintenance of BMP-2 expression in adult human articular chondrocytes. This finding differed from a previously reported result with epiphyseal chondrocytes showing that the inhibition of NF-κB strongly reduced the expression of BMP-2 in the growth plates (24). On the other hand, the inhibitor suppressed the induction of BMP-2 by TNF-α by ~50%. The suppressive effect seemed to reach a plateau at a concentration of 100 μM, because no further suppression was observed with a higher concentration of PDTC. In contrast, when SB203580 was used together with PDTC, the induction was completely abrogated, and the expression of BMP-2 declined below the level of endogenous expression. Although PDTC partly suppressed BMP-2 induction, the inhibitor did not change the stability of BMP-2 mRNA in TNF-α-treated chondrocytes (Fig. 7*B*), suggesting the possibility that the induction was suppressed not through a change in post-transcriptional regulation, but rather through the decrease in transcriptional activity.

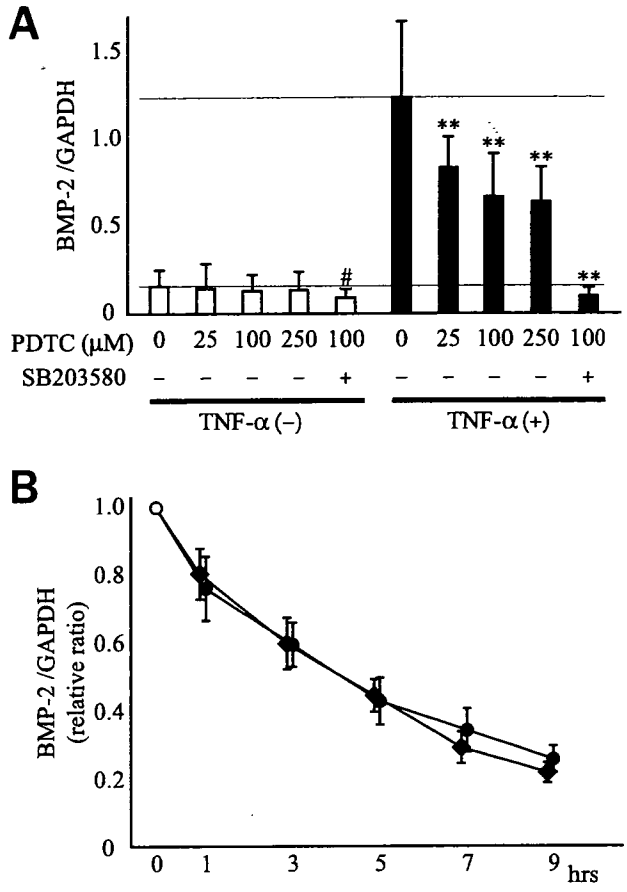

FIGURE 7. **Involvement of NF-κB in induction of BMP-2.** *A*, effect of PDTC on endogenous expression and induction of BMP-2 by TNF-α was evaluated in primary cultured human articular chondrocytes. In presence or absence of TNF-α, PDTC was given to chondrocytes at various concentrations. For some cells, SB203580 (20 μM) was given together with PDTC. Forty-eight hours later, expression of BMP-2 was evaluated by real-time PCR and represented by ratios against GAPDH. #, $p < 0.05$ against untreated cells, and **, $p < 0.01$ against cells treated with TNF-α alone. *B*, stability of BMP-2 mRNA was evaluated using ActD (1 μM) in chondrocytes treated with TNF-α for 48 h with (*filled diamonds*) or without (*filled circles*) PDTC (100 μM). At each time point, expression of BMP-2 was determined by real-time PCR together with GAPDH, and their RNA ratio was obtained. To facilitate direct comparison, ratios at respective time points were normalized by the ratio at beginning of the evaluation (*i.e.* Time 0) under each experimental condition. For these experiments, TNF-α was used at a concentration of 100 ng/ml. Data are shown by mean ± S.D. or mean ± S.D. of three to five experiments.

FIGURE 6. **Involvement of p38 MAP kinase in the induction of BMP-2 by TNF-α.** *A*, human articular chondrocytes were maintained by monolayer culture, and seven specific inhibitors of signal transduction pathways were examined at indicated concentrations to determine whether they exerted significant effects on endogenous expression and induction of BMP-2 by TNF-α. Effects on endogenous expression were evaluated 48 h after addition of inhibitors. To assess effects on induction, inhibitors were given 30 min prior to addition of TNF-α to media, and induction levels were determined 48 h later. Expression of BMP-2 was represented by ratios against GAPDH. #, $p < 0.05$; ##, $p < 0.01$ against control cells; *, $p < 0.05$; **, $p < 0.01$ against control cells treated with TNF-α alone. *B*, chondrocytes were cultured with graded doses of SB203580 in the presence (*solid bars*) or absence (*open bars*) of TNF-α stimulation, and the expression of BMP-2 was evaluated 48 h later. In parallel, the effect of SB202190 on the expression of BMP-2 was evaluated together with that of SB202474, a negative control for the p38 inhibitors (*bars in shaded areas*). Expression of BMP-2 was represented by ratios against GAPDH. #, $p < 0.05$, and ##, $p < 0.01$ against untreated cells; **, $p < 0.01$ against cells treated with TNF-α alone. *C*, chondrocytes were cultured for 48 h in the presence (*open squares*) or absence (*open circles*) of SB203580, and the stability of BMP-2 mRNA was evaluated using ActD (1 μM). Evaluation was also performed on cells treated with TNF-α for 48 h with (*filled squares*) or without (*filled circles*) SB203580. To facilitate direct comparison, RNA ratios at respective time points were normalized by the ratio at beginning of the evaluation (*i.e.* Time 0) under each experimental condition. *D* and *E*, chondrocytes were infected with the adenovirus carrying constitutively active MKK6 at indicated titers, and 72 h later, the amount of phosphorylated p38 and expression of BMP-2 mRNA were evaluated together with those of total p38 protein and GAPDH, respectively. SB203580 was given to some cells together with the adenovirus. In *E*, BMP-2 expression was represented by ratios against GAPDH. **, $p < 0.01$ against untreated cells. For these experiments, expression of BMP-2 and GAPDH was quantitatively evaluated by real-time PCR. TNF-α was used at the concentration of 100 ng/ml, and media containing inhibitors were replaced every 24 h to preclude possible degradation of the inhibitors. Data are shown by mean ± S.D. or mean ± S.D. of three or four experiments.

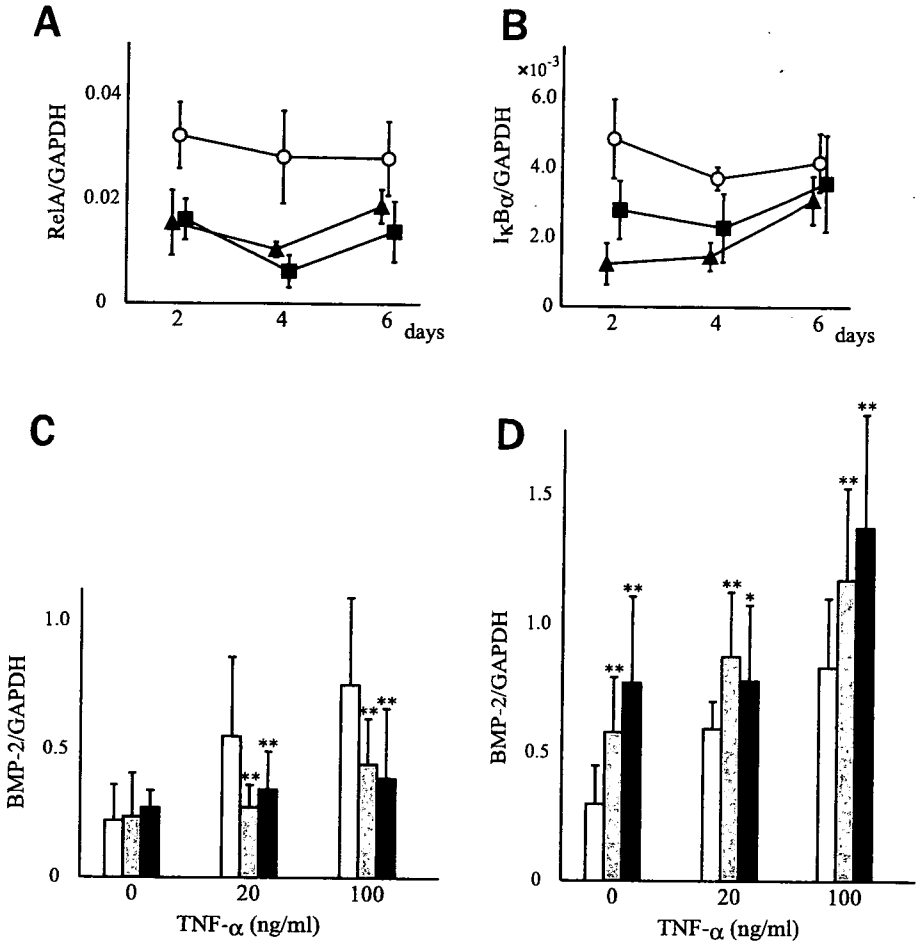

FIGURE 8. **Influence of reduced RelA and IκBα expression on the induction of BMP-2 by TNF-α.** *A* and *B*, siRNAs for RelA (*A*) and IκBα (*B*) were delivered into primary cultured human chondrocytes by electroporation, and the expression levels of respective genes were monitored every 2 days until Day 6 by real-time PCR. For each gene, two siRNAs with respective target sequences were used (*filled squares* and *triangles*), and the results are shown by ratios against GAPDH together with that of the control cells given a control siRNA (*open circles*). *C* and *D*, the cells to which the siRNAs for RelA (*C*) and IκBα (*D*) were delivered were treated with 20 or 100 ng/ml of TNF-α for 48 h, and the induction of BMP-2 was evaluated by real-time PCR. Considering the time course of gene suppression, the cells were treated with TNF-α from Day 2 to Day 4. *Open bars* represent the result of control cells, and *light* and *dark shaded bars* show the results of respective siRNAs used for the gene. The results are shown by ratios against GAPDH. *, $p < 0.05$ and **, $p < 0.01$ against control cells in respective treatment groups. Data are mean ± S.D. or mean ± S.D. of three to five experiments.

Induction of BMP-2 by TNF-α Was Significantly Modulated by the Suppression of RelA and IκBα Expression—The involvement of NF-κB in the induction of BMP-2 was further confirmed by RNAi experiments. In primary cultured human articular chondrocytes, the expression of RelA and IκBα was effectively reduced by RNAi. The result of real-time PCR demonstrated that the expression of RelA gene was suppressed from Day 2 to Day 6 after the delivery of siRNAs into the cells (Fig. 8*A*). The strongest inhibition was observed at Day 4 for both siRNAs used for the gene, when the expression levels were reduced to 22 and 37%, respectively, of that of the control. For IκBα, the suppression was strongest at Day 2 and Day 4 for respective siRNAs, when the expression was 25 and 44% of the control (Fig. 8*B*). Next, the induction of BMP-2 by TNF-α was evaluated in the cells given the siRNAs. The introduction of siRNA by electroporation considerably reduced the induction of BMP-2 by TNF-α (Fig. 8, *C* and *D*). Nonetheless, it was noticed that the gene silencing of RelA significantly inhibited the induction of BMP-2 (Fig. 8*C*). Meanwhile, the reduction of IκBα expression caused a ~2-fold increase of endogenous BMP-2 expression (Fig. 8*D*). The response to TNF-α was preserved in those cells, although the magnitude of BMP-2 induction was not augmented by the suppression of IκBα.

Noggin Showed Stronger Inhibitory Effects on Chondrocyte Anabolism after TNF-α Treatment—To evaluate the biological significance of BMP-2 induced by TNF-α, cartilage explants were cultured in the presence or absence of the cytokine, and the inhibitory effect of noggin on the synthetic activity of chondrocytes in those explants was investigated. In this experiment, the concentration of TNF-α was set at a relatively low level based on our previous experience (12). First, the induction of BMP-2 by TNF-α was confirmed by immunostaining. Compared with the untreated controls (Fig. 9*A*), staining for BMP-2 was much stronger in the TNF-α-treated explants (Fig. 9*B*). In those explants, the staining was observed both inside and around the chondrocytes, which was consistent with our previous observation with human cartilage explants (12). Next, the synthesis of sulfated proteoglycan in the explants was evaluated by the incorporation of [^{35}S]sulfate. In the control explants without TNF-α treatment, the incorporation of [^{35}S]sulfate into the explants was not significantly influenced by the addition of noggin to the culture media (Fig. 9*C*). On the other hand, noggin showed a strong inhibitory effect on the explants treated with TNF-α. Although the low dose of cytokine did not cause significant suppression of the synthetic activity in the explants, noggin reduced the incorporation of [^{35}S]sulfate by >50%. Thus, in the TNF-α-treated explants, BMP-2 induced by TNF-α was considered to play a significant anabolic role on the synthetic activity of chondrocytes, likely counteracting the suppressive effects of TNF-α.

DISCUSSION

In the current work, the presence of a complex regulation for BMP-2 expression was initially suggested in ATDC5 cells by the experiment using CHX. The expression of BMP-2 was induced by CHX in differentiated but not undifferentiated ATDC5 cells, whereas the basal level of BMP-2 expression was consistently low throughout the differentiation process. Because CHX is known to induce gene expression through the inhibition of RNA degradation (35), that observation suggested the possibil-

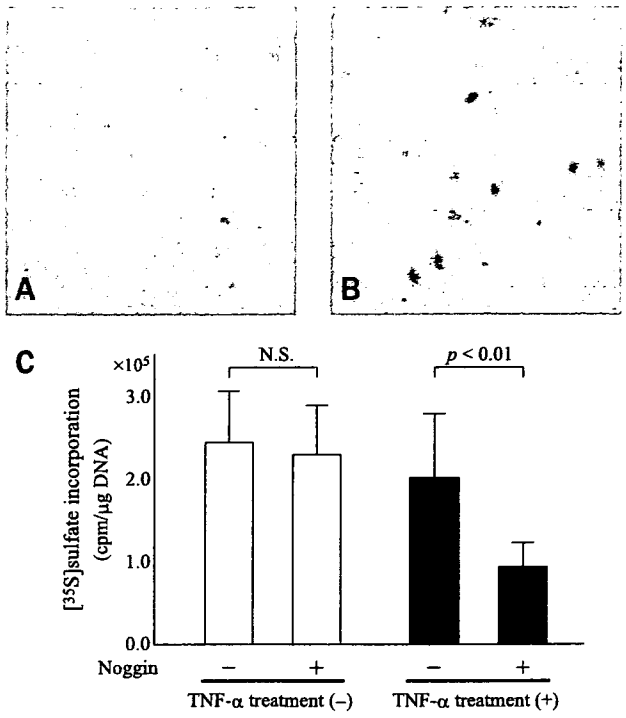

FIGURE 9. **Expression of BMP-2 and effect of noggin on sulfate incorporation in cartilage explants with and without TNF-α treatment.** *A* and *B*, cartilage explants were cultured in the presence or absence of TNF-α (2.5 ng/ml) for 4 days, and the expression of BMP-2 was detected by immunostaining. Representative photomicrographs of the control explants without TNF-α treatment (*A*) and those treated with TNF-α (*B*) are shown. Magnification, ×200. *C*, the explants with and without TNF-α treatment were further cultured for 2 days in the presence or absence of recombinant mouse noggin (1 μg/ml), and the synthetic activity of chondrocytes was evaluated by the incorporation of [^{35}S]sulfate into the explants. The experiments were repeated four times using cartilage from two animals. *Open bars* represent the results of the explants without TNF-α treatment, and *solid bars* represent for those with TNF-α treatment. The results are shown as cpm normalized by DNA contents. Data are mean ± S.D.

ity that BMP-2 mRNA was synthesized at a certain level in differentiated cells, even without TNF-α stimulation. Accordingly, the results of nuclear run-off experiments revealed that differentiated ATDC5 cells were in fact synthesizing BMP-2 mRNA at the nuclei, whereas such synthesis was barely detectable in undifferentiated cells. The discrepancy between the active mRNA synthesis in the nuclei and the low level of expression observed in differentiated cells can be explained by the involvement of post-transcriptional control in the regulation of BMP-2 expression. On the other hand, the results of nuclear run-off experiments also revealed that the transcriptional activity of BMP-2 mRNA was increased by TNF-α. Taking all these results into account, the regulation of BMP-2 in ATDC5 cells may be understood as follows. In undifferentiated cells, expression is suppressed at the transcriptional level. The cells acquire the ability to synthesize BMP-2 mRNA with the progression of chondrogenic differentiation, but the overall expression is still suppressed by a post-transcriptional regulatory mechanism that facilitates mRNA degradation. TNF-α induces the expression of BMP-2 in differentiated cells through the transcriptional up-regulation and stabilization of mRNA. The regulatory mechanisms were then investigated in primary cultured human chondrocytes, and the results of those experiments indicated that human chondrocytes most likely have a similar regulatory system for the control of BMP-2 expression.

In eukaryotic cells, the level of gene expression is strictly regulated at both transcriptional and post-transcriptional levels. Modulation of the mRNA decay rate is a strategy widely used by cells to adjust the intensity of expression (44). The decay of mRNA is often mediated by the specific *cis*-acting sequences in 3′-UTR, represented by an AU-rich element or ARE (29, 45). The ARE often contains multiple copies of pentameric AUUUA motifs. Such motifs have been found in many unstable and inducible genes such as cytokines and oncogenes, where the elements control the degeneration of mRNA in response to a variety of intra- and extracellular signals, enabling a rapid adjustment of RNA levels (46). In the present study, the result of 3′-rapid amplification of cDNA ends revealed that both human and mouse BMP-2 mRNA contain multiple AUUUA motifs in the 3′-UTRs. Mouse 3′-UTR contains 8 motifs within a proximal 320-nt AU-rich stretch, and their alignment is highly conserved in the human gene. In various genes whose expression is regulated at the post-transcriptional level, the nucleotide sequences of AREs are often evolutionarily conserved (47–50). The result of this study indicated that BMP-2 could be one such gene. Because BMP-2 protein is highly conserved during the evolutionary process, it is reasonable to assume that the regulatory mechanism is conserved as well. In fact, a sequence comparison has revealed that a 265-nucleotide region in the BMP-2 3′-UTR is 73% conserved over a span of 450 million years of evolution from fish to mammals (27). Interestingly, with all its functional and sequential similarity to BMP-2, the BMP-4 gene lacks an equivalent conserved region in the 3′-UTR. The possible absence of post-transcriptional regulation may account for the difference in the expression patterns between the two BMPs during embryogenesis (5, 17, 18).

Although AREs regulate the decay of mRNA in many genes, the presence of ARE in 3′-UTR does not necessarily indicate that the element is actually functional (45). Furthermore, the significance of AREs may vary depending on the cell types (51) or states of cellular differentiation (21, 27, 45, 52), possibly due to the change in trans-acting regulators (45). Thus, the function of ARE needs to be evaluated within the biological context in which the gene is expressed. In this study, we therefore examined the function of BMP-2 3′-UTR in differentiated ATDC5 cells, in which the addition of 3′-UTR to the luciferase gene did indeed reduce the enzyme activity. That reduction was related to the number of inserted AUUUA motifs, rather than to the specific sequence in the region. Thus, out of eight pentameric motifs, the first or last two pentamers alone did not change the luciferase activity significantly, whereas the middle four within 86 bases suppressed it by over 40%. The addition of two motifs, either proximal or distal, was enough to obtain suppression equal to the entire 3′-UTR.

AREs are often divided into three classes, with the ARE of BMP-2 falling into class II, in which the region is characterized by multiple copies of clustered AUUUA motifs (53, 54). The other members of this class are mostly cytokines and enzymes such as interleukin-3 (40), TNF-α (55), and cyclooxygenese-2 (51, 56, 57). In these genes, the effect of mRNA stabilization by

the pentameric sequence has often been related to the number of motifs in the AREs (40, 57). Our current observations are in good agreement with those previous results.

It is worth noting that a few previous studies reported contradictory results on whether or not the addition of 3′-UTR increased the stability of BMP-2 mRNA (21, 27). Considering that AREs primarily destabilize rather than stabilize mRNA (29, 36, 44, 45), it is possible that the previous observations might not reflect the actual function of the 3′-UTR *in vivo*. Because an embryonic carcinoma cell line was used in those studies, the inconsistency might stem from differences in the cell types and/or stages of cellular differentiation. Because the reduced luciferase activity by the addition of 3′-UTR was significantly recovered by TNF-α, we think the current result reasonably reflects the biological function of the region.

Based on the results of our current study, it seems very likely that the p38 signal pathway mediates the stabilization of BMP-2 mRNA by TNF-α. In genes containing AREs, the stability of mRNA is regulated by proteins that bind to the region or ARE-binding proteins. The function of such proteins is often modulated by the p38 signal pathway. For example, the ARE-binding proteins HuR, AUF1, and tristetraprolin are all known to stabilize or destabilize mRNA in response to p38 signaling (42, 58–60). Although the protein that binds to BMP-2 ARE has not been determined, it is likely that mRNA stability is regulated by one such protein. AREs regulated by the p38 pathway have a common feature in that they contain several closely adjacent AUUUA motifs (36). That feature is indeed shared with the BMP-2 gene.

Besides the post-transcriptional regulation, the modulation of transcriptional activity seemed to play another important role in the induction of BMP-2 by TNF-α. In differentiated ATDC5 cells, TNF-α increased the transcriptional rate of BMP-2, whereas in human cells, the induction of BMP-2 was partly suppressed by an NF-κB inhibitor without changing the stability of mRNA. The involvement of NF-κB in the induction of BMP-2 was further suggested by the result of RNAi experiment. In the present study, the reduction of RelA expression by RNAi strongly suppressed the induction of BMP-2 by TNF-α. In the meantime, because neither addition of PDTC nor suppression of RelA changed the level of endogenous BMP-2 expression, it is assumed that the transcriptional factor may not play a significant role in the maintenance of BMP-2 in the untreated chondrocytes. This speculation is consistent with the result that the suppression of IκBα by RNAi caused significant elevation of endogenous BMP-2 expression. The evidence that the expression of BMP-2 is transcriptionally regulated by NF-κB has been shown in a previous study in the growth plate chondrocytes (24), and our current results indicated that the transcriptional regulation could be involved in the induction of BMP-2 by TNF-α in articular chondrocytes, together with the mRNA stabilization mechanism.

The induction of BMP-2 in chondrocytes could be a critical factor in several pathologies, *e.g.* osteoarthritis. In osteoarthritis joints, the anabolic activity of the chondrocytes is highly up-regulated, which likely retards disease progression (61). In osteoarthritis cartilage, the expression of BMP-2 is significantly increased (12, 15), possibly through the induction by the pro-inflammatory cytokines (12). Because the protein has potent anabolic actions on chondrocytes (62, 63), it is possible that the induced BMP-2 counteracts the progression of the disease by enhancing the chondrocyte metabolism. In fact, the result of this study indicated a possibility that BMP-2, after induction by TNF-α, could compensate the reduced chondrocyte metabolism caused by the cytokine (Fig. 9). The notion is also supported by a recent observation that mice lacking a BMP receptor in cartilage tended to develop premature osteoarthritis (64).

Thus, for pathologies that involve BMP-2 expression, its control could be a key to regulating the disease process. The results of this study will provide useful clues in developing new strategies to treat various diseases involving chondrocytes.

REFERENCES

1. Urist, M. R. (1965) *Science* **150,** 893–899
2. Wozney, J. M., Rosen, V., Celeste, A. J., Mitsock, L. M., Whitters, M. J., Kriz, R. W., Hewick, R. M., and Wang, E. A. (1988) *Science* **242,** 1528–1534
3. Sampath, T. K., Rashka, K. F., Doctor, J. S., Tucker, R. F., and Hoffmann, F. M. (1993) *Proc. Natl. Acad. Sci. U. S. A.* **90,** 6004–6008
4. Zhang, H., and Bradley, A. (1996) *Development* **122,** 2977–2986
5. Hogan, B. L. (1996) *Genes Dev.* **10,** 1580–1594
6. Pizette, S., and Niswander, L. (2000) *Dev. Biol.* **219,** 237–249
7. Bostrom, M. P., Lane, J. M., Berberian, W. S., Missri, A. A., Tomin, E., Weiland, A., Doty, S. B., Glaser, D., and Rosen, V. M. (1995) *J. Orthop. Res.* **13,** 357–367
8. Si, X., Jin, Y., Yang, L., Tipoe, G. L., and White, F. H. (1997) *Eur. J. Oral Sci.* **105,** 325–330
9. Hallahan, A. R., Pritchard, J. I., Chandraratna, R. A. S., Ellenbogen, R. G., Geyer, J. R., Overland, R. P., Strand, A. D., Topcott, S. J., and Olson, J. M. (2003) *Nat. Med.* **9,** 1033–1038
10. Kleeff, J., Maruyama, H., Ishiwata, T., Sawhney, H., Friess, H., Buchler, M. W., and Korc, M. (1999) *Gastroenterology* **116,** 1202–1216
11. Langenfeld, E. M., Calvano, S. E., Abou-Nukta, F., Lowry, S. F., Amenta, P., and Langenfeld, J. (2003) *Carcinogenesis* **24,** 1445–1454
12. Fukui, N., Zhu, Y., Maloney, W. J., Clohisy, J., and Sandell, L. J. (2003) *J. Bone Joint Surg. Am.* **85A,** Suppl. 3, 59–66
13. van Lent, P. L., Blom, A. B., van der Kraan, P., Holthuysen, A. E., Vitters, E., van Rooijen, N., Smeets, R. L., Nabbe, K. C., and van den Berg, W. B. (2004) *Arthritis Rheum.* **50,** 103–111
14. Lories, R. J., Derese, I., Ceuppens, J. L., and Luyten, F. P. (2003) *Arthritis Rheum.* **48,** 2807–2818
15. Nakase, T., Miyaji, T., Tomita, T., Kaneko, M., Kuriyama, K., Myoui, A., Sugamoto, K., Ochi, T., and Yoshikawa, H. (2003) *Osteoarthritis Cartilage* **11,** 278–284
16. Zoricic, S., Maric, I., Bobinac, D., and Vukicevic, S. (2003) *J. Anat.* **202,** 269–277
17. Lyons, K. M., Pelton, R. W., and Hogan, B. L. (1989) *Genes Dev.* **3,** 1657–1668
18. Lyons, K. M., Pelton, R. W., and Hogan, B. L. (1990) *Development* **109,** 833–844
19. Macias, D., Gañan, Y., Sampath, T. K., Piedra, M. E., Ros, M. A., and Hurle, J. M. (1997) *Development* **124,** 1109–1117
20. Zhang, D., Ferguson, C. M., O'Keefe, R. J., Puzas, J. E., Roiser, R. N., and Reynolds, P. R. (2002) *J. Bone Miner. Res.* **17,** 293–300
21. Abrams, K. L., Xu, J., Nativelle-Serpentini, C., Dabirshahsahebi, S., and Rogers, M. B. (2004) *J. Biol. Chem.* **279,** 15916–15928
22. Boylan, J. F., Lufkin, T., Achkar, C. C., Taneja, R., Chambon, P., and Gudas, L. J. (1995) *Mol. Cell. Biol.* **15,** 843–851
23. Helvering, L. M., Sharp, R. L., Ou, X., and Geiser, A. G. (2000) *Gene (Amst.)* **256,** 123–138
24. Feng, J. Q., Xing, L., Zhang, J.-H., Zhao, M., Horn, D., Chan, J., Boyce, B. F., Harris, S. E., Mundy, G. R., and Chen, D. (2003) *J. Biol. Chem.* **278,** 29130–29135
25. Zhou, S., Turgeman, G., Harris, S. E., Leitman, D. C., Komm, B. S., Bodine,

P. V. N., and Gazit, D. (2003) *Mol. Endocrinol.* **17,** 56–66
26. Ghosh-Choudhury, N., Choudhury, C. G., Harris, M. A., Wozney, J., Mundy, G. R., Abboud, S. L., and Harris, S. E. (2001) *Biochem. Biophys. Res. Commun.* **286,** 101–108
27. Fritz, D. T., Liu, D., Xu, J., Jiang, S., and Rogers, M. B. (2004) *J. Biol. Chem.* **279,** 48950–48958
28. St Johnston, D. (1995) *Cell* **81,** 161–170
29. Mignone, F., Gissi, C., Liuni, S., and Pesole, G. (2002) *Genome Biology* http://genomebiology.com/2002/3/3/reviews/0004
30. Shi, J., Schmitt-Talbot, E., DiMattia, D. A., and Dullea, R. G. (2004) *Inflamm. Res.* **53,** 377–389
31. Fowler, M. J., Jr., Neff, M. S., Borghaei, R. C., Pease, E. A., Mochan, E., and Thornton, R. D. (1998) *Biochem. Biophys. Res. Commun.* **248,** 450–453
32. Atsumi, T., Miwa, Y., Kimata, K., and Ikawa, Y. (1990) *Cell Differ. Dev.* **30,** 109–116
33. Kuettner, K. E., Pauli, B. U., Gall, G., Memoli, V. A., and Schenk, R. K. (1982) *J. Cell Biol.* **93,** 743–750
34. Seto, H., Kamekura, S., Miura, T., Yamamoto, A., Chikuda, H., Ogata, T., Hiraoka, H., Oda, H., Nakamura, K., Kurosawa, H., Chung, U.-I., Kawaguchi, H., and Tanaka, S. (2004) *J. Clin. Invest.* **113,** 718–726
35. Beelman, C. A., and Parker, R. (1994) *J. Biol. Chem.* **269,** 9687–9692
36. Dean, J. L. E., Sully, G., Clark, A. R., and Saklatvala, J. (2004) *Cell. Signal.* **16,** 1113–1121
37. Esnault, S., and Malter, J. S. (2002) *Blood* **99,** 4048–4052
38. Shaw, G., and Kamen, R. (1986) *Cell* **46,** 659–667
39. Chen, C. Y., Gherzi, R., Andersen, J. S., Gaietta, G., Jurchott, K., Royer, H. D., Mann, M., and Karin, M. (2000) *Genes Dev.* **14,** 1236–1248
40. Ming, X. F., Kaiser, M., and Moroni, C. (1998) *EMBO J.* **17,** 6039–6048
41. Short, S., Tian, D., Short, M. L., and Jungmann, R. A. (2000) *J. Biol. Chem.* **275,** 12963–12969
42. Ming, X. F., Stoecklin, G., Lu, M., Looser, R., and Moroni, C. (2001) *Mol. Cell. Biol.* **21,** 5778–5789
43. Stoecklin, G., Hahn, S., and Moroni, C. (1994) *J. Biol. Chem.* **269,** 28591–28597
44. Wilusz, C. J., Wormington, M., and Peltz, S. W. (2001) *Nat. Rev. Mol. Cell. Biol.* **2,** 237–246
45. Bevilacqua, A., Ceriani, M. C., Capaccioli, S., and Nicolin, A. (2003) *J. Cell. Physiol.* **195,** 356–372
46. Saklatvala, J., Dean, J., and Clark, A. (2003) *Biochem. Soc. Symp.* **70,** 95–106
47. Asson-Batres, M. A., Spurgeon, S. L., Diaz, J., DeLoughery, T. G., and Bagby, H. C., Jr. (1994) *Proc. Natl. Acad. Sci. U. S. A.* **91,** 1318–1322
48. Dorssers, L., Burger, H., Bot, F., Delwel, R., Geurts van Kessel, A. H., Lowenberg, B., and Wagemaker, G. (1987) *Gene (Amst.)* **55,** 115–124
49. Schiavone, N., Rosini, P., Quattrone, A., Donnini, M., Lapucci, A., Citti, L., Bevilacqua, A., Nicolin, A., and Capaccioli, S. (2000) *FASEB J.* **14,** 174–184
50. Vasudevan, S., and Peltz, S. W. (2001) *Mol. Cell* **7,** 1191–1200
51. Cox, S. J., and Morrison, A. R. (2001) *J. Biol. Chem.* **276,** 23179–23185
52. Bashirullah, A., Cooperstock, R. L., and Lipshitz, H. D. (2001) *Proc. Natl. Acad. Sci. U. S. A.* **98,** 7025–7028
53. Chen, C. Y., Xu, N., and Shyu, A. B. (1995) *Mol. Cell. Biol.* **15,** 5777–5788
54. Peng, S. S., Chen, Y., and Shyu, A. B. (1996) *Mol. Cell. Biol.* **16,** 1490–1499
55. Brook, M., Sully, G., Clark, A. R., and Saklatvala, J. (2000) *FEBS Lett.* **483,** 57–61
56. Dean, J. L., Brook, M., Clark, A. R., and Saklatvala, J. (1999) *J. Biol. Chem.* **274,** 264–269
57. Dixon, D. A., Kaplan, C. D., McIntyre, T. M., Zimmerman, G. A., and Prescott, S. M. (2000) *J. Biol. Chem.* **275,** 11750–11757
58. Carballo, E., Chao, H., Lai, W. S., Kennington, E. A., Campbell, D., and Blackshear, P. J. (2001) *J. Biol. Chem.* **276,** 42580–42587
59. Dean, J. L., Wait, R., Mahtani, K. R., Sully, G., Clark, A. R., and Saklatvala, J. (2001) *Mol. Cell. Biol.* **21,** 721–730
60. Wilson, G. M., Lu, J., Sutphen, K., Sun, Y., Huynh, Y., and Brewer, G. (2003) *J. Biol. Chem.* **278,** 33029–33038
61. Sandell, L. J., and Aigner, T. (2001) *Arthritis Res.* **3,** 107–113
62. Grunder, T., Gaissmaier, C., Fritz, J., Stoop, R., Hortschansky, P., Mollenhauer, J., and Aicher, W. K. (2004) *Osteoarthritis Cartilage* **12,** 559–567
63. Stewart, M. C., Saunders, K. M., Burton-Wurster, N., and Macleod, J. N. (2000) *J. Bone Miner. Res.* **15,** 166–174
64. Rountree, R. B., Schoor, M., Chen, H., Marks, M. E., Harley, V., Mishina, Y., and Kingley, D. M. (2004) *PLoS Biol.* **2,** e335 http://www.plosbiology.org. doi:10.1371/journal.pbio.0020355

Effects of CD44 antibody– or RGDS peptide–immobilized magnetic beads on cell proliferation and chondrogenesis of mesenchymal stem cells

Shinobu Yanada,[1] Mitsuo Ochi,[1] Nobuo Adachi,[1] Hiroo Nobuto,[1] Muhammad Agung,[1] Seiichi Kawamata[2]
[1]*Department of Orthopaedic Surgery, Graduate School of Biomedical Sciences, Hiroshima University, Hiroshima, 734-8551, Japan*
[2]*Department of Anatomy, Graduate School of Health Sciences, Hiroshima University, Hiroshima, 734-8551, Japan*

Received 14 June 2005; revised 18 September 2005; accepted 5 October 2005
Published online 24 March 2006 in Wiley InterScience (www.interscience.wiley.com). DOI: 10.1002/jbm.a.30635

Abstract: We evaluated the efficacy of a novel mesenchymal stem cell (MSC) delivery system using an external magnetic field for cartilage repair *in vitro*. MSCs were isolated from the bone marrow of Sprague Drawley rats and expanded in a monolayer. To use the MSC delivery system, two types of MSC-magnetic bead complexes were designed and compared. Expanded MSCs were combined with small-sized (diameter: 310 nm) carboxyl group-combined (0.01–0.04 μmol/mg) magnetic beads, Ferri Sphere 100C®, through either anti-rat CD44 mouse monoclonal antibodies or a synthetic cell adhesion factor, arginine (R)-glycine (G)-aspartic acid (D)-serine (S) (RGDS) peptide. Both cell complexes were successfully created, and were able to proliferate in monolayer culture up to at least day 7 after separation of magnetic beads from the cell surface, although the proliferation of the complexes was slower in the early period of culture than that of non-labeled rat MSCs (after 7 days of culture: proliferation of CD44 antibody-bead complexes, approximately 50%; RGDS peptide-bead complexes, 70% versus non-labeled rat MSCs, respectively). These complexes were seeded onto culture plates with or without an external magnetic force (magnetic flux density was 0.20 Tesla at a distance of 2 mm from plate base) generated by a neodymium magnet, and supplemented with chondrogenic differentiation medium. Both complexes could be attached and gathered effectively under the influence of the external magnet, and CD44-bead complexes could effectively generate chondrogenic matrix in monolayer culture. In a three-dimensional culture system, the production of a dense chondrogenic matrix and the expression of type II collagen and aggrecan mRNA were detected in both complexes, and the chondrogenic potential of these complexes was only a little less than that of rat MSCs alone. Thus, we conclude that due to the fact that MSC-RGDS peptide-bead complexes are composed using a biodegradable material, RGDS peptide, as a mediator, the RGDS peptide-bead complex is more useful for minimally invasive clinical applications using our design of magnetic MSC delivery system than CD44 antibody-beads. © 2006 Wiley Periodicals, Inc. J Biomed Mater Res 77A: 773–784, 2006

Key words: magnetic beads; magnetic force; mesenchymal stem cell; cell proliferation; chondrogenic differentiation

INTRODUCTION

Regenerative medicine for tissue repair has been the focus of many studies. In the field of orthopedics, the expectation of regenerative medicine for cartilage repair has been increasing, because articular cartilage has poor intrinsic healing capacity due to a lack of blood vessels and its isolation from the systemic regulation.[1–3] Although much work on regenerative medicine is currently focused on tissue engineering, this usually requires technically demanding procedures with some special equipment or facilities and proper scaffolds or growth factors. Therefore, intravenous or intraarticular cell transplantation without scaffolds is a more attractive option, for repair. However, one problem with the injection of isolated cells is the fact that they are likely to be easily diluted in the joint fluid, and they probably cannot reside in the injured site for the required period for tissue regeneration.

To solve the aforementioned problem, we attempted to develop a technique for cell-based cartilage repair in which cells were coupled with magnetic beads. Cells coupled with magnetic beads were in-

Correspondence to: M. Ochi, Department of Orthopaedic Surgery, Graduate School of Biomedical Sciences, Hiroshima University, 1–2-3 Kasumi, Minami-Ku, Hiroshima, 734-8551, Japan; e-mail: ochim@hiroshima-u.ac.jp

Contract grant sponsor: Ministry of Education, Culture, Sports, Science and Technology of Japan; contract grant number: 16209045

jected into a joint, and external magnetic fields were used to localize the transplanted cells at the desired location.[4] For transplanted cells, bone marrow-derived mesenchymal stem cells (MSCs) were used, because it is well known that under the appropriate conditions they can differentiate into several lineages, including osteogenic, chondrogenic, or adipogenic lineages[5] and MSCs, when cultured with buffy coat and red blood cells from bone marrow after isolation without cell separation using a density gradient, express specific surface antigen molecules such as CD29 and CD44.[6] Recently, Majumdar et al. have reported that CD44 on CD105-positive bone marrow stromal cells, including MSCs showing the ability to proliferate and differentiate along the chondrogenic lineage, is expressed at ~98% of the level of freshly isolated cells up to at least passage five.[7] Based on this information, we hypothesized that CD44-positive bone marrow-derived MSCs cultured by Kotobuki's method (which is easier than Majumdar's isolation method) would have the ability to proliferate and differentiate along the chondrogenic lineage. To verify this hypothesis and use our magnetic cell delivery system for cartilage repair, anti-CD44 antibodies were chosen as a mediator to couple cells with magnetic beads. Following a successful pilot study using CD44-antibody-immobilized magnetic bead-conjugated MSCs developed by us (MSC-CD44 antibody-magnetic-bead complex),[4] we report here on further experiments using this complex.

In addition, most cells including MSCs express integrin proteins in the cell membrane, and attach to extracellular matrix proteins, such as fibronectin, through the cell adhesion factor, arginine (R)-glycine (G)-aspartic acid (D) (RGD) amino acid sequence.[8–10] MSCs also express integrin αv, which is one of the ligands of RGD peptides,[11] and are known to be adhesive cells.[5–7] Subsequent to our design of the MSC-CD44 antibody-magnetic-bead complex, we wished to assemble an MSC-magnetic bead complex, using a more biodegradable material than antibodies as the mediator, because antibodies are thought to be difficult to degrade in the body as binding between the antigen and the antibody is strong. We, therefore, also combined MSCs with a synthetic cell adhesion factor, RGD-serine (S), to generate (RGDS) peptide-immobilized magnetic beads (MSC-RGDS peptide-magnetic-bead complex).

To use our magnetic cell delivery system for cartilage repair, the present study set out to investigate the effects of the two materials (CD44 antibody- or RGDS peptide-immobilized magnetic beads) on cell proliferation, the delivery to the desired location by external magnetic field, and the chondrogenic potential of MSCs, and to verify *in vitro* which material is most useful for our magnetic cell delivery system.

MATERIALS AND METHODS

Isolation and expansion of mesenchymal stem cells (MSCs)

Experimental rats were kept in the research facilities for laboratory animal science at our university. The research protocol of this experiment was reviewed and approved by the university ethical committee. The method of isolation and *in vitro* expansion of bone marrow-derived MSCs, retaining the phenotype, is well known and has been previously described.[6] A modification of Kotobuki's culture method was used. Briefly, bone marrow from Sprague Dawley (SD) rats (12-weeks-old) was flushed out of the marrow cavities, using a pressurized culture medium consisting of high glucose-Dulbecco's modified Eagle's medium (DMEM, Invitrogen Corp., Carlsbad, CA) with 10% heat-inactivated fetal bovine serum (FBS, Sigma–Aldrich Corp., St. Louis, MO) and penicillin-streptomycin-fungizone (Bio-Whittaker, ML). The cells including buffy coat and red blood cells were seeded onto 100-mm culture dishes (Falcon, BD Bioscience, Franklin Lakes, NJ) in culture medium, and incubated in a humidified atmosphere of 5% CO_2–95% air at 37°C. The medium remained unchanged for the first 7 days, and was subsequently changed every 2–3 days. Two to 3 weeks after seeding, the cells had proliferated and reached confluence. The cells were then harvested by treating with 0.25% trypsin and 0.02% EDTA, and rinsed twice with culture medium. To expand the MSCs, 2–3 × 10^5 of the harvested cells were seeded on 100-mm culture dishes. On reaching confluence again, the cells were reseeded under the same conditions.

Expression of the cell surface antigen, CD44, in MSCs (immunohistochemical staining)

To examine whether rat MSCs expanded in monolayer culture express the surface antigen, CD44, immunohistochemical staining was performed. About 3 × 10^4 MSCs were attached to a glass slide by centrifugation, dried, and fixed with ethanol for 30 min. To avoid a non-specific reaction, the prepared specimens were treated with Histofine® blocking reagent (Nichirei Co., Tokyo, Japan). The specimens were then treated with anti-rat CD44 mouse monoclonal antibodies (Chemicon International Inc, Temecula, CA) at a final concentration of 1 μg/mL in 3% bovine serum albumin (BSA, Sigma) in phosphate buffered saline without calcium and magnesium (PBS(−)) at 4°C overnight in a humidified atmosphere. Biotin-labeled anti-mouse secondary antibody (Nichirei) was applied for 10 min at 25°C, followed by alkaline phosphatase-labeled streptavidin (Nichirei) treatment for 10 min. Finally, the specimens were incubated with alkaline phosphatase substrate solution (color development: fast red, Nichirei) for 20 min at 25°C, and the nuclei were counterstained with Haematoxylin. The specimens were examined with a Nicon light microscope. Controls were treated following the same procedure, except that the primary antibody was omitted.